DESY-13-153
December 2013

Precise Calculation of the Dilepton Invariant-Mass Spectrum and the Decay Rate in $B^\pm \to \pi^\pm \mu^+ \mu^-$ in the SM

Ahmed Ali[1]

Theory Group, Deutsches Elektronen-Synchrotron DESY, D-22603 Hamburg, FRG.

Alexander Ya. Parkhomenko[2] **& Aleksey V. Rusov**[3]

Department of Theoretical Physics, P. G. Demidov Yaroslavl State University, Sovietskaya 14, 150000 Yaroslavl, Russia.

We present a precise calculation of the dilepton invariant-mass spectrum and the decay rate for $B^\pm \to \pi^\pm \ell^+ \ell^-$ ($\ell^\pm = e^\pm, \mu^\pm$) in the Standard Model (SM) based on the effective Hamiltonian approach for the $b \to d \ell^+ \ell^-$ transitions. With the Wilson coefficients already known in the next-to-next-to-leading logarithmic (NNLL) accuracy, the remaining theoretical uncertainty in the short-distance contribution resides in the form factors $f_+(q^2)$, $f_0(q^2)$ and $f_T(q^2)$. Of these, $f_+(q^2)$ is well measured in the charged-current semileptonic decays $B \to \pi \ell \nu_\ell$ and we use the B-factory data to parametrize it. The corresponding form factors for the $B \to K$ transitions have been calculated in the Lattice-QCD approach for large-q^2 and extrapolated to the entire q^2-region using the so-called z-expansion. Using an $SU(3)_F$-breaking Ansatz, we calculate the $B \to \pi$ tensor form factor, which is consistent with the recently reported lattice $B \to \pi$ analysis obtained at large q^2. The prediction for the total branching fraction $\mathcal{B}(B^\pm \to \pi^\pm \mu^+ \mu^-) = (1.88^{+0.32}_{-0.21}) \times 10^{-8}$ is in good agreement with the experimental value obtained by the LHCb collaboration. In the low q^2-region, the Heavy-Quark Symmetry (HQS) relates the three form factors with each other. Accounting for the leading-order symmetry-breaking effects, and using data from the charged-current process $B \to \pi \ell \nu_\ell$ to determine $f_+(q^2)$, we calculate the dilepton invariant-mass distribution in the low q^2-region in the $B^\pm \to \pi^\pm \ell^+ \ell^-$ decay. This provides a model-independent and precise calculation of the partial branching ratio for this decay.

[1]E-mail: ahmed.ali@desy.de
[2]E-mail: parkh@uniyar.ac.ru
[3]E-mail: rusov@uniyar.ac.ru

1 Introduction

Recently, the LHCb collaboration has reported the first observation of the $B^\pm \to \pi^\pm\mu^+\mu^-$ decay, using 1.0 fb^{-1} integrated luminosity in proton-proton collisions at the Large Hadron Collider (LHC) at $\sqrt{s} = 7$ TeV [1]. Unlike the $b \to s\,\ell^+\ell^-$ transitions, which have been studied at the B-factories and hadron colliders in a number of decays, such as $B \to (K,\,K^*)\,\ell^+\ell^-$ and $B_s \to \phi\,\ell^+\ell^-$ [2], the $B^\pm \to \pi^\pm\,\mu^+\mu^-$ decay is the first $b \to d\,\ell^+\ell^-$ transition measured so far. Phenomenological analysis of this process, under controlled theoretical errors, will provide us independent information concerning the $b \to d$ Flavor-Changing-Neutral-Current (FCNC) transitions in the B-meson sector. Hence, $B^\pm \to \pi^\pm\mu^+\mu^-$ decay is potentially an important input in the precision tests of the SM in the flavor sector and, by the same token, also in searches for physics beyond it.

The measured branching ratio $\mathcal{B}(B^+ \to \pi^+\mu^+\mu^-) = [2.3 \pm 0.6(\text{stat}) \pm 0.1(\text{syst})] \times 10^{-8}$ [1] is in good agreement with the SM expected rate [3], which, however, like a number of other estimates in the literature [4, 5], is based on model-dependent input for the $B \to \pi$ form factors. The Light-Cone Sum Rules (LCSR) approach (see, for example, [6] and [7]) is certainly helpful in the low q^2-region and has been used in the current phenomenological analysis of the data [1]. However, theoretical accuracy of the LCSR-based form factors is limited due to the dependence on numerous input parameters and wave function models. Hence, it is very desirable to calculate the form factors from first principles, such as Lattice-QCD, which have their own range of validity restricted by the recoil energy (here, the energy E_π of the π-meson), as the discretization errors become large with increasing E_π. With improved lattice technology, one can use the lattice form factors to predict the decay rates in the $B \to \pi$ and $B \to K$ transitions (as well as in other heavy-to-light meson transitions) in the low-recoil region, where the lattice results apply without any extrapolation, in a model-independent manner. At present, the dimuon invariant mass distribution in the $B^+ \to \pi^+\,\mu^+\mu^-$ decay is not at hand and only the integrated branching ratio is known. We combine the lattice input with other phenomenologically robust approaches to calculate the dilepton invariant-mass spectrum in the entire q^2-region to compute the corresponding integrated decay rates for comparison with the data [1]. Our framework makes use of the methods based on the Heavy-Quark Symmetry (HQS) in the large-recoil region, data from the B-factory experiments on the charged-current processes[4] $B^0 \to \pi^-\ell^+\nu_\ell$ and $B^+ \to \pi^0\ell^+\nu_\ell$ to determine one of the form factors, $f_+(q^2)$, and the available lattice results on the $B \to \pi$ and $B \to K$ form factors in the low-recoil region.

We recall that the decay $B^\pm \to \pi^\pm\,\ell^+\ell^-$ involves three form factors, two of which, $f_+(q^2)$ and $f_0(q^2)$, characterize the hadronic $B \to \pi$ matrix element of the vector current $J_V^\mu(x) = \bar{b}(x)\gamma^\mu d(x)$, and the third, $f_T(q^2)$, enters in the corresponding matrix element of the tensor current $J_T^\mu(x) = \bar{b}(x)\sigma^{\mu\nu}q_\nu d(x)$, where $q^\mu = p_B^\mu - p_\pi^\mu$ is the momentum transferred to the lepton pair $\ell^+\ell^-$ (see Eqs. (15) and (16) below). Using isospin symmetry, the first two form factors are the same as the ones encountered in the charged-current processes $B^+ \to \pi^0\ell^+\nu_\ell$ and $B^0 \to \pi^-\ell^+\nu_\ell$. Of these, the contribution to the decay rate

[4] Charge conjugation is implicit in this paper.

proportional to $f_0(q^2)$ is strongly suppressed by the mass ratio m_ℓ^2/m_B^2 (for $\ell = e,\, \mu$). The form factor $f_+(q^2)$ has been well measured (modulo $|V_{ub}|$) in the entire q^2-range by the BaBar [8,9] and Belle [10,11] collaborations. We have undertaken a chi-squared fit of these data, using four popular form-factor parametrizations of $f_+(q^2)$: (i) the Becirevic-Kaidalov (BK) parametrization [12], (ii) the Ball-Zwicky (BZ) parametrization [6], (iii) the Boyd-Grinstein-Lebed (BGL) parametrization [13], and (iv) the Bourrely-Caprini-Lellouch (BCL) parametrization [14]. All these parametrizations yield good fits measured in terms of $\chi^2_{\rm min}/{\rm ndf}$, where ndf is the number of degrees of freedom (see Table 3). However, factoring in theoretical arguments based on the Soft-Collinear Effective Theory (SCET) [15], and preference of the Lattice-QCD-based analysis of the form factors $f_+(q^2)$, $f_0(q^2)$, and $f_T(q^2)$ in terms of the so-called z-expansion, and a variation thereof (see Ref. [16] for a recent summary of the lattice heavy-to-light form factors), we use the BGL-parametrization as our preferred choice for the extraction of $f_+(q^2)$ from the $B \to \pi \ell \nu_\ell$ data.

In order to determine the other two form factors, $f_0(q^2)$ and $f_T(q^2)$, in the entire q^2-domain, we proceed as follows: Lattice QCD provides them in the high-q^2 region. A number of dedicated lattice-based studies of the heavy-to-light form factors are available in the literature. In particular, calculations of the form factors in the $B \to (K,\, K^*)\, \ell^+\ell^-$ decays, based on the $2+1$ flavor gauge configurations generated by the MILC collaboration [17], have been undertaken by the FNAL/MILC [18, 19], HPQCD [20, 21] and the Cambridge/Edinburgh [22,23] Lattice groups. We make use of the $B \to K$ lattice results, combining them with an Ansatz on the $SU(3)_F$-symmetry breaking to determine the $f_T(q^2)$ form factor for the $B \to \pi$ transition. Very recently, new results on the $B \to \pi$ form factors, in particular the first preliminary results on the tensor form factor $f_T^{B\pi}(q^2)$, from the lattice simulations have also become available [24, 25]. While the analysis presented in Ref. [25] by the FermiLab Lattice and MILC Collaborations is still blinded with an unknown off-set factor, promised to be disclosed when the final results are presented, we use the available results on the $f_T^{BK}(q^2)$ form factor by the HPQCD collaboration [20,21] as input in the high q^2-region to constrain our Ansatz on the $SU(3)_F$-symmetry breaking. Thus, combining the extraction of $f_+(q^2)$ from the $B \to \pi \ell \nu_\ell$ data, the lattice-QCD data on $f_T(q^2)$ for the large-q^2 domain, and the BGL-like parametrization [13] in the form of z-expansion to extrapolate this form factor to the lower q^2-range, we obtain the following branching ratio:

$$\mathcal{B}(B^+ \to \pi^+ \mu^+ \mu^-) = (1.88^{+0.32}_{-0.21}) \times 10^{-8} \,, \tag{1}$$

which has a combined accuracy of about $\pm 15\%$, taking into account also the uncertainties in the CKM matrix elements, for which we have used the values obtained from the fits of the CKM unitarity triangle [26]. This result is in agreement (within large experimental errors) with the experimental value reported recently by the LHCb collaboration [1]:

$$\mathcal{B}(B^+ \to \pi^+ \mu^+ \mu^-) = (2.3 \pm 0.6({\rm stat.}) \pm 0.1({\rm syst.})) \times 10^{-8}. \tag{2}$$

As the lattice calculations of the $B \to \pi$ form factors become robust and the dilepton invariant-mass spectrum in $B^+ \to \pi^+ \mu^+ \mu^-$ is measured, one can undertake a completely quantitative fit of the data in the SM taking into account correlations in the lattice calculations and data.

In the SM, $b \to d\,\ell^+\ell^-$ transition is suppressed essentially by the factor $|V_{td}/V_{ts}|$ relative to the $b \to s\,\ell^+\ell^-$ transition. In terms of exclusive decays, first measurement of the ratio $\mathcal{B}(B^+ \to \pi^+\ell^+\ell^-)/\mathcal{B}(B^+ \to K^+\ell^+\ell^-)$ has been reported by the LHCb collaboration [1]:

$$\frac{\mathcal{B}(B^+ \to \pi^+\mu^+\mu^-)}{\mathcal{B}(B^+ \to K^+\mu^+\mu^-)} = 0.053 \pm 0.014(\text{stat.}) \pm 0.001(\text{syst.})\ . \tag{3}$$

In the SM, this ratio can be expressed as follows:

$$\frac{\mathcal{B}(B^+ \to \pi^+\mu^+\mu^-)}{\mathcal{B}(B^+ \to K^+\mu^+\mu^-)} = \left|\frac{V_{td}}{V_{ts}}\right|^2 F_{\text{tot}}^{\pi/K}\ , \tag{4}$$

where $F_{\text{tot}}^{\pi/K}$ is the ratio resulting from the convolution of the form factors and the q^2-dependent effective Wilson coefficients. Using $F_{\text{tot}}^{\pi/K} = 0.87$, and neglecting the errors on this quantity, LHCb has determined the ratio of the CKM matrix elements, yielding $|V_{td}/V_{ts}| = 0.266 \pm 0.035(\text{stat.}) \pm 0.003(\text{syst.})$ [1]. At present this method is not competitive with other determinations of $|V_{td}/V_{ts}|$, such as from the $B_{(s)}$–$\bar{B}_{(s)}$ mixings [2], but with greatly improved statistical error, anticipated at the LHC and Super-B factory experiments, this would become a valuable and independent constraint on the CKM matrix. A reliable estimate of the quantity $F_{\text{tot}}^{\pi/K}$ is also required. In particular, we expect that the error on the corresponding quantity, $F_{\text{HQS}}^{\pi/K}(q^2 \le q_0^2)$, denoting the ratio of the partial branching ratios restricted to the low-q^2-domain, can be largely reduced with the help of the heavy quark symmetry (HQS). We hope to return to improved theoretical estimates of $F_{\text{tot}}^{\pi/K}$ and $F_{\text{HQS}}^{\pi/K}(q^2 \le q_0^2)$ in a future publication.

In the large-recoil limit, the form factors in the $B \to (\pi,\, \rho,\, \omega)$ and $B \to (K,\, K^*)$ transitions obey heavy quark symmetry, reducing the number of independent form factors [27]. In particular, the $B \to \pi$ form factors $f_0(q^2)$ and $f_T(q^2)$ are related to $f_+(q^2)$ in the HQS limit (see Eqs. (67) and (68) below). Taking into account the leading-order symmetry-breaking corrections, these relations get modified [28], bringing in their wake a dependence on the QCD coupling constant $\alpha_s(\mu_h)$ and $\alpha_s(\mu_{hc})$, where the hard scale $\mu_h \simeq m_b$ and the intermediate (or hard-collinear) scale $\mu_{hc} = \sqrt{m_b\Lambda}$, with $\Lambda \simeq 0.5$ GeV, reflect the multi-scale nature of this problem. In addition, a non-perturbative quantity ΔF_π, which involves the leptonic decay constants f_B and f_π and the first inverse moments of the leading-twist light-cone distribution amplitudes (LCDAs) of the B- and π-meson also enters (see Eqs. (73) and (74) below). We have used the HQS-based approach to determine the $f_T(q^2)$ form factor in terms of the measured $f_+(q^2)$ form factor from the semileptonic $B \to \pi\ell\nu_\ell$ data, discussed above. This provides a model-independent determination of the dilepton invariant-mass distribution in the low q^2-region.

Uncertainties from the form factors aside, the other main problem from the theoretical point of view in the $b \to d\,\ell^+\ell^-$ transitions is the so-called long-distance contributions, which are dominated by the $\bar{c}c$ and $\bar{u}u$ resonant states which show up as charmonia (J/ψ, $\psi(2S)$, ...) and light vector (ρ and ω) mesons, respectively. Only model-dependent descriptions (in a Breit-Wigner form) of such long-distance effects are known at present, which compromise the precision in the theoretical predictions of the total branching fractions. Excluding the resonance-dominated regions from the dilepton invariant-mass distributions is therefore the preferred way to compare data and theory. With this in mind, we calculate the following partially integrated branching ratio

$$\mathcal{B}(B^+ \to \pi^+\mu^+\mu^-;\, 1\,\mathrm{GeV}^2 \le q^2 \le 8\,\mathrm{GeV}^2) = \left(0.57^{+0.07}_{-0.05}\right) \times 10^{-8}\ , \tag{5}$$

where the lower and upper q^2-value boundaries are chosen to remove the light-vector (ρ- and ω-mesons) and charmonium-resonant regions. However, with the product branching ratios [26]: $\mathcal{B}(B^+ \to \rho^0\pi^+) \times \mathcal{B}(\rho^0 \to \mu^+\mu^-) = (3.78 \pm 0.59) \times 10^{-10}$ and $\mathcal{B}(B^+ \to \omega\pi^+) \times \mathcal{B}(\omega \to \mu^+\mu^-) = (6.2 \pm 2.2) \times 10^{-10}$, the long-distance effects in the low q^2-region are numerically not important.

Due to the small branching ratio, it will be a while before the entire dimuon invariant mass is completely measured in the $B^+ \to \pi^+\,\mu^+\mu^-$ decay. Anticipating this, and following similar procedures adopted in the analysis of the data in the $B \to (K,\, K^*)\,\ell^+\ell^-$ decays [29,30] we present here results for the partial branching ratios $d\mathcal{B}(B^+ \to \pi^+\mu^+\mu^-)/dq^2$, binned over specified ranges $[q^2_{\rm min}, q^2_{\rm max}]$ in eight q^2-intervals. They would allow the experiments to check the short-distance (renormalization-improved perturbative) part of the SM contribution in the $b \to d\,\ell^+\ell^-$ transitions precisely.

This paper is organized as follows: In Section 2, we present the dilepton invariant-mass spectrum $d\mathcal{B}(B^+ \to \pi^+\,\mu^+\mu^-)/dq^2$ in the effective Hamiltonian approach based on the SM and the numerical values of the effective Wilson coefficients. Section 3 is devoted to the four popular parameterizations of the vector, scalar and tensor form factors. Section 4 describes the fits of the semileptonic data on the $B \to \pi\ell\nu_\ell$ decays using the form-factor parametrizations discussed earlier. Section 5 describes the calculation of the form factors $f_0(q^2)$ and $f_T(q^2)$ for the $B \to \pi$ transition, using Lattice data as input in the high q^2-region and the z-expansion to extrapolate it to low-q^2. Section 6 contains the calculation of the dilepton invariant-mass spectrum in the low-q^2 region, using methods based on the Heavy-Quark Symmetry. In Section 7, we present the dilepton invariant-mass spectrum in the entire q^2-region as well as the partial decay rates, integrated over eight different q^2-intervals. A summary and outlook are given in Section 8.

2 The $B^+ \to \pi^+\ell^+\ell^-$ Decay

The effective weak Hamiltonian encompassing the transitions $b \to d\,\ell^+\ell^-$ ($\ell^\pm = e^\pm,\, \mu^\pm$, or $\tau^\pm$), in the Standard Model (SM) can be written as follows [31]:

$$\mathcal{H}_{\rm eff}^{b\to d} = \frac{4G_F}{\sqrt{2}} \left[V_{ud}V_{ub}^* \left(C_1\,\mathcal{O}_1^{(u)} + C_2\,\mathcal{O}_2^{(u)} \right) + V_{cd}V_{cb}^* \left(C_1\,\mathcal{O}_1 + C_2\,\mathcal{O}_2 \right) - V_{td}V_{tb}^* \sum_{i=3}^{10} C_i\,\mathcal{O}_i \right], \tag{6}$$

where G_F is the Fermi constant, $V_{q_1q_2}$ are the CKM matrix elements which satisfy the unitary condition $V_{ud}V_{ub}^* + V_{cd}V_{cb}^* + V_{td}V_{tb}^* = 0$ (it can be used to eliminate one combination). In contrast to the $b \to s$ transition, all three terms in the unitarity relation are of the same order in λ ($V_{ub}^*V_{ud} \sim V_{cb}^*V_{cd} \sim V_{tb}^*V_{td} \sim \lambda^3$), with $\lambda = \sin\theta_{12} \simeq 0.2232$ [26].

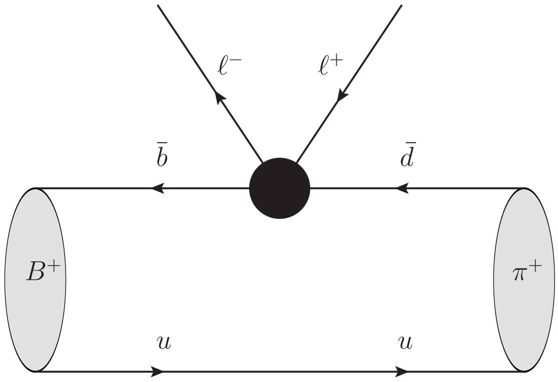

Figure 1: Feynman diagram for the decay $B^+ \to \pi^+\ell^+\ell^-$.

The local operators appearing in (6) are the dimension-six operators, and are defined at an arbitrary scale μ as follows [32, 33]:

$$\mathcal{O}_1^{(u)} = \left(\bar{d}_L\gamma_\mu T^A u_L\right)\left(\bar{u}_L\gamma^\mu T^A b_L\right), \qquad \mathcal{O}_2^{(u)} = \left(\bar{d}_L\gamma_\mu u_L\right)\left(\bar{u}_L\gamma^\mu b_L\right), \tag{7}$$

$$\mathcal{O}_1 = \left(\bar{d}_L\gamma_\mu T^A c_L\right)\left(\bar{c}_L\gamma^\mu T^A b_L\right), \qquad \mathcal{O}_2 = \left(\bar{d}_L\gamma_\mu c_L\right)\left(\bar{c}_L\gamma^\mu b_L\right), \tag{8}$$

$$\mathcal{O}_3 = \left(\bar{d}_L\gamma_\mu b_L\right)\textstyle\sum_q\left(\bar{q}\gamma^\mu q\right), \qquad \mathcal{O}_4 = \left(\bar{d}_L\gamma_\mu T^A b_L\right)\textstyle\sum_q\left(\bar{q}\gamma^\mu T^A q\right), \tag{9}$$

$$\mathcal{O}_5 = \left(\bar{d}_L\gamma_\mu\gamma_\nu\gamma_\rho b_L\right)\textstyle\sum_q\left(\bar{q}\gamma^\mu\gamma^\nu\gamma^\rho q\right), \quad \mathcal{O}_6 = \left(\bar{d}_L\gamma_\mu\gamma_\nu\gamma_\rho T^A b_L\right)\textstyle\sum_q\left(\bar{q}\gamma^\mu\gamma^\nu\gamma^\rho T^A q\right), \tag{10}$$

$$\mathcal{O}_7 = \frac{e\, m_b}{g_s^2}\left(\bar{d}_L\sigma^{\mu\nu} b_R\right) F_{\mu\nu}, \qquad \mathcal{O}_8 = \frac{m_b}{g_s}\left(\bar{d}_L\sigma^{\mu\nu} T^A b_R\right) G^A_{\mu\nu} \tag{11}$$

$$\mathcal{O}_9 = \frac{e^2}{g_s^2}\left(\bar{d}_L\gamma^\mu b_L\right)\sum_\ell\left(\bar{\ell}\gamma_\mu\ell\right), \qquad \mathcal{O}_{10} = \frac{e^2}{g_s^2}\left(\bar{d}_L\gamma^\mu b_L\right)\sum_\ell\left(\bar{\ell}\gamma_\mu\gamma_5\ell\right), \tag{12}$$

where e is the electric elementary charge, g_s is the strong coupling, $i,\ j = 1, 2, 3$ are the color indices of quarks, $\sigma_{\mu\nu} = i\left(\gamma_\mu\gamma_\nu - \gamma_\nu\gamma_\mu\right)/2$, the subscripts L and R refer to the left- and right-handed components of the fermion fields, $\psi_{L,R} = (1 \mp \gamma_5)\,\psi/2$, $F_{\mu\nu}$ and $G^A_{\mu\nu}$ are the photon and gluon fields, respectively, and m_b is the b-quark mass. (The terms in the operators $\mathcal{O}_7$ and $\mathcal{O}_8$ proportional to the d-quark mass m_d are omitted as their contributions to the amplitudes are suppressed by the ratio $m_d/m_b \sim 10^{-3}$ and negligible at the present level of accuracy). Sums over q and ℓ denote sums over all quarks (except the t-quark) and charged leptons, respectively.

The Wilson coefficients $C_i(\mu)$ $(i = 1, \ldots, 10)$ depending on the renormalization scale μ are calculated at the matching scale $\mu_W \sim M_W$, the W-boson mass, as a perturbative expansion in the strong coupling constant $\alpha_s(\mu_W)$ [33]:

$$C_i(\mu_W) = C_i^{(0)}(\mu_W) + \frac{\alpha_s(\mu_W)}{4\pi}\, C_i^{(1)}(\mu_W) + \left(\frac{\alpha_s(\mu_W)}{4\pi}\right)^2 C_i^{(2)}(\mu_W) + \ldots, \tag{13}$$

and can be evolved to a lower scale $\mu_b \sim m_b$ using the anomalous dimensions of the above operators to NNLL order [33]:

$$\gamma_i = \frac{\alpha_s(\mu_W)}{4\pi}\,\gamma_i^{(0)} + \left(\frac{\alpha_s(\mu_W)}{4\pi}\right)^2 \gamma_i^{(1)} + \left(\frac{\alpha_s(\mu_W)}{4\pi}\right)^3 \gamma_i^{(2)} + \dots . \tag{14}$$

Feynman diagram of the decay $B^+ \to \pi^+\ell^+\ell^-$ is displayed in Fig. 1 in which the solid blob represents the effective Hamiltonian $\mathcal{H}_{\rm eff}^{b\to d}$ (6). The hadronic matrix elements of the operators $\mathcal{O}_i$ between the B- and π-meson states are expressed in terms of three independent form factors [34]:

$$\langle\pi(p_\pi)|\bar{b}\gamma^\mu d|B(p_B)\rangle = f_+(q^2)\left[p_B^\mu + p_\pi^\mu - \frac{m_B^2-m_\pi^2}{q^2}\,q^\mu\right] + f_0(q^2)\,\frac{m_B^2-m_\pi^2}{q^2}\,q^\mu, \tag{15}$$

$$\langle\pi(p_\pi)|\bar{b}\sigma^{\mu\nu}q_\nu d|B(p_B)\rangle = \frac{i f_T(q^2)}{m_B+m_\pi}\left[q^2\left(p_B^\mu+p_\pi^\mu\right) - \left(m_B^2-m_\pi^2\right)q^\mu\right], \tag{16}$$

where p_B^μ and p_π^μ are the four-momenta of the B- and π-mesons, respectively, m_B and m_π are their masses, and $q^\mu = p_B^\mu - p_\pi^\mu$ is the momentum transferred to the lepton pair. The $B\to\pi$ transition form factors $f_+(q^2)$, $f_0(q^2)$ and $f_T(q^2)$ are scalar functions whose shapes are determined by using non-perturbative methods. Of these, using the isospin symmetry, $f_+(q^2)$ can also be obtained by performing a phenomenological analysis of the existing experimental data on the charged-current semileptonic decays $B\to\pi\ell\nu_\ell$. In the large-recoil (low-q^2) limit, these form factors are related by the heavy-quark symmetry, as discussed below.

The differential branching fraction in the dilepton invariant mass q^2 can be expressed as follows:

$$\frac{d\mathcal{B}\left(B^+\to\pi^+\ell^+\ell^-\right)}{dq^2} = \frac{G_F^2\alpha_{\rm em}^2\tau_B}{1024\pi^5 m_B^3}\,|V_{tb}V_{td}^*|^2\sqrt{\lambda(q^2)}\sqrt{1-\frac{4m_\ell^2}{q^2}}\,F(q^2), \tag{17}$$

where $\alpha_{\rm em}$ is the fine-structure constant, m_ℓ is the lepton mass, τ_B is the B-meson lifetime,

$$\lambda(q^2) = \left(m_B^2+m_\pi^2-q^2\right)^2 - 4m_B^2 m_\pi^2 \tag{18}$$

is the kinematic function encountered in three-body decays (the triangle function), and $F(q^2)$ is the dynamical function encoding the Wilson coefficients and the form factors:

$$\begin{aligned} F(q^2) &= \frac{2}{3}\,\lambda(q^2)\left(1+\frac{2m_\ell^2}{q^2}\right)\left|C_9^{\rm eff}(q^2)\,f_+(q^2) + \frac{2m_b}{m_B+m_\pi}\,C_7^{\rm eff}(q^2)\,f_T(q^2)\right|^2 \\ &+ \frac{2}{3}\,\lambda(q^2)\left(1-\frac{4m_\ell^2}{q^2}\right)\left|C_{10}^{\rm eff}\,f_+(q^2)\right|^2 + \frac{4m_\ell^2}{q^2}\left(m_B^2-m_\pi^2\right)^2\left|C_{10}^{\rm eff}\,f_0(q^2)\right|^2 . \end{aligned} \tag{19}$$

Note that the last term in Eq. (19) containing the form factor $f_0(q^2)$ is strongly suppressed by the mass ratio m_ℓ^2/q^2 for the electron or muon pair production over the most of the dilepton invariant-mass spectrum and will not be needed in our numerical estimates. The dynamical function (19) contains the effective Wilson coefficients $C_7^{\rm eff}(q^2)$, $C_9^{\rm eff}(q^2)$

and $C_{10}^{\rm eff}$ which are specific combinations of the Wilson coefficients entering the effective Hamiltonian (6). To the NNLO approximation, the effective Wilson coefficients are given by [33, 35–38]:

$$
\begin{aligned}
C_7^{\rm eff}(q^2) &= A_7 - \frac{\alpha_s(\mu)}{4\pi}\left[C_1^{(0)}F_1^{(7)}(s) + C_2^{(0)}F_2^{(7)}(s) + A_8^{(0)}F_8^{(7)}(s)\right] && (20)\\
&+ \lambda_u \frac{\alpha_s(\mu)}{4\pi}\left[C_1^{(0)}\left(F_{1,u}^{(7)}(s) - F_1^{(7)}(s)\right) + C_2^{(0)}\left(F_{2,u}^{(7)}(s) - F_2^{(7)}(s)\right)\right], \\
C_9^{\rm eff}(q^2) &= A_9 + T_9\, h(m_c^2, q^2) + U_9\, h(m_b^2, q^2) + W_9\, h(0, q^2) && (21)\\
&- \frac{\alpha_s(\mu)}{4\pi}\left[C_1^{(0)}F_1^{(9)}(s) + C_2^{(0)}F_2^{(9)}(s) + A_8^{(0)}F_8^{(9)}(s)\right] \\
&+ \lambda_u \left(\frac{4}{3}\, C_1(\mu) + C_2(\mu)\right)\left[h(m_c^2, q^2) - h(0, q^2)\right] \\
&+ \lambda_u \frac{\alpha_s(\mu)}{4\pi}\left[C_1^{(0)}\left(F_{1,u}^{(9)}(s) - F_1^{(9)}(s)\right) + C_2^{(0)}\left(F_{2,u}^{(9)}(s) - F_2^{(9)}(s)\right)\right], \\
C_{10}^{\rm eff} &= \frac{4\pi}{\alpha_s(\mu)}\, C_{10}(\mu), && (22)
\end{aligned}
$$

where $s = q^2/m_B^2$ is the reduced momentum squared of the lepton pair. The quantity λ_u above is the ratio of the CKM matrix elements, defined as follows:

$$
\lambda_u \equiv \frac{V_{ub}V_{ud}^*}{V_{tb}V_{td}^*} = -\frac{R_b}{R_t}\, e^{i\alpha}, \tag{23}
$$

which is expressed in terms of the apex angle α and the sides $R_t = \sqrt{(1-\bar\rho)^2 + \bar\eta^2}$ and $R_b = \sqrt{\bar\rho^2 + \bar\eta^2}$ [26] of the unitarity triangle, where $\bar\rho$ and $\bar\eta$ are the perturbatively improved Wolfenstein parameters [39] of the CKM matrix. The usual procedure is to include an additional term usually denoted by $Y(q^2)$ [37, 40] into the $C_9^{\rm eff}(q^2)$ Wilson coefficient (21) which effectively accounts for the resonant states (mostly charmonia decaying into the lepton pair). But, as stated in the introduction, we only concentrate on the short-distance part in the differential branching ratio.

Following the prescription of Ref. [37], the terms $\omega_i(s)$ accounting for the bremsstrahlung corrections necessary for the inclusive $B \to (X_s,\, X_d)\, \ell^+\ell^-$ decays are omitted and, the

Table 1: Wilson coefficients C_1, C_2, $C_{10}^{\rm eff}$, and the combinations of the Wilson coefficients specified in Eqs. (24)–(29), are shown at three representative renormalization scales: $\mu_b = 2.45$ GeV, $\mu_b = 4.90$ GeV and $\mu_b = 9.80$ GeV. The strong coupling $\alpha_s(\mu)$ is evaluated by the three-loop expression in the $\overline{\rm MS}$ scheme with five active flavors and $\alpha_s(M_Z) = 0.1184$ [26]. The entries correspond to the top-quark mass $m_t = 175$ GeV. The superscript (0) denotes the lowest order contribution while a quantity with the superscript (1) is a perturbative correction of order α_s, and $X = X^{(0)} + X^{(1)}$.

	$\mu = 2.45$ GeV	$\mu = 4.90$ GeV	$\mu = 9.80$ GeV
$\alpha_s(\mu)$	0.269	0.215	0.180
$(C_1^{(0)}, C_1^{(1)})$	(−0.707, 0.241)	(−0.492, 0.207)	(−0.330, 0.184)
$(C_2^{(0)}, C_2^{(1)})$	(1.047, −0.028)	(1.024, −0.017)	(1.011, 0.010)
$(A_7^{(0)}, A_7^{(1)})$	(−0.355, 0.025)	(−0.313, 0.010)	(−0.278, −0.001)
$A_8^{(0)}$	−0.164	−0.148	−0.134
$(A_9^{(0)}, A_9^{(1)})$	(4.299, −0.237)	(4.171, −0.053)	(4.164, 0.090)
$(T_9^{(0)}, T_9^{(1)})$	(0.101, 0.280)	(0.367, 0.251)	(0.571, 0.231)
$(U_9^{(0)}, U_9^{(1)})$	(0.046, 0.023)	(0.033, 0.015)	(0.023, 0.010)
$(W_9^{(0)}, W_9^{(1)})$	(0.045, 0.016)	(0.032, 0.012)	(0.022, 0.008)
$(C_{10}^{{\rm eff}(0)}, C_{10}^{{\rm eff}(1)})$	(−4.560, 0.378)	(−4.560, 0.378)	(−4.560, 0.378)

following set of auxiliary functions is used:

$$
\begin{aligned}
A_7(\mu) &= \frac{4\pi}{\alpha_s(\mu)}\,C_7(\mu) - \frac{1}{3}\,C_3(\mu) - \frac{4}{9}\,C_4(\mu) - \frac{20}{3}\,C_5(\mu) - \frac{80}{9}\,C_6(\mu), && (24)\\
A_8(\mu) &= \frac{4\pi}{\alpha_s(\mu)}\,C_8(\mu) + C_3(\mu) - \frac{1}{6}\,C_4(\mu) + 20\,C_5(\mu) - \frac{10}{3}\,C_6(\mu), && (25)\\
A_9(\mu) &= \frac{4\pi}{\alpha_s(\mu)}\,C_9(\mu) + \sum_{i=1}^{6} C_i(\mu)\,\gamma_{i9}^{(0)}\,\ln\frac{m_b}{\mu} + \frac{4}{3}\,C_3(\mu) + \frac{64}{9}\,C_5(\mu) + \frac{64}{27}\,C_6(\mu), && (26)\\
T_9(\mu) &= \frac{4}{3}\,C_1(\mu) + C_2(\mu) + 6\,C_3(\mu) + 60\,C_5(\mu), && (27)\\
U_9(\mu) &= -\frac{7}{2}\,C_3(\mu) - \frac{2}{3}\,C_4(\mu) - 38\,C_5(\mu) - \frac{32}{3}\,C_6(\mu), && (28)\\
W_9(\mu) &= -\frac{1}{2}\,C_3(\mu) - \frac{2}{3}\,C_4(\mu) - 8\,C_5(\mu) - \frac{32}{3}\,C_6(\mu), && (29)
\end{aligned}
$$

where the required elements of the anomalous dimension matrix $\gamma_{ij}^{(0)}$ can be read off from Ref. [33]. The numerical values of the scale-dependent functions specified above at three representative scales $\mu = 2.45$ GeV, $\mu = 4.90$ GeV and $\mu = 9.80$ GeV are presented in Table 1. In Eq. (21) m_c and m_b are the c- and b-quark masses, respectively, the masses of the light u-, d-, and s-quarks are neglected, and the standard one-loop function $h(z, s)$

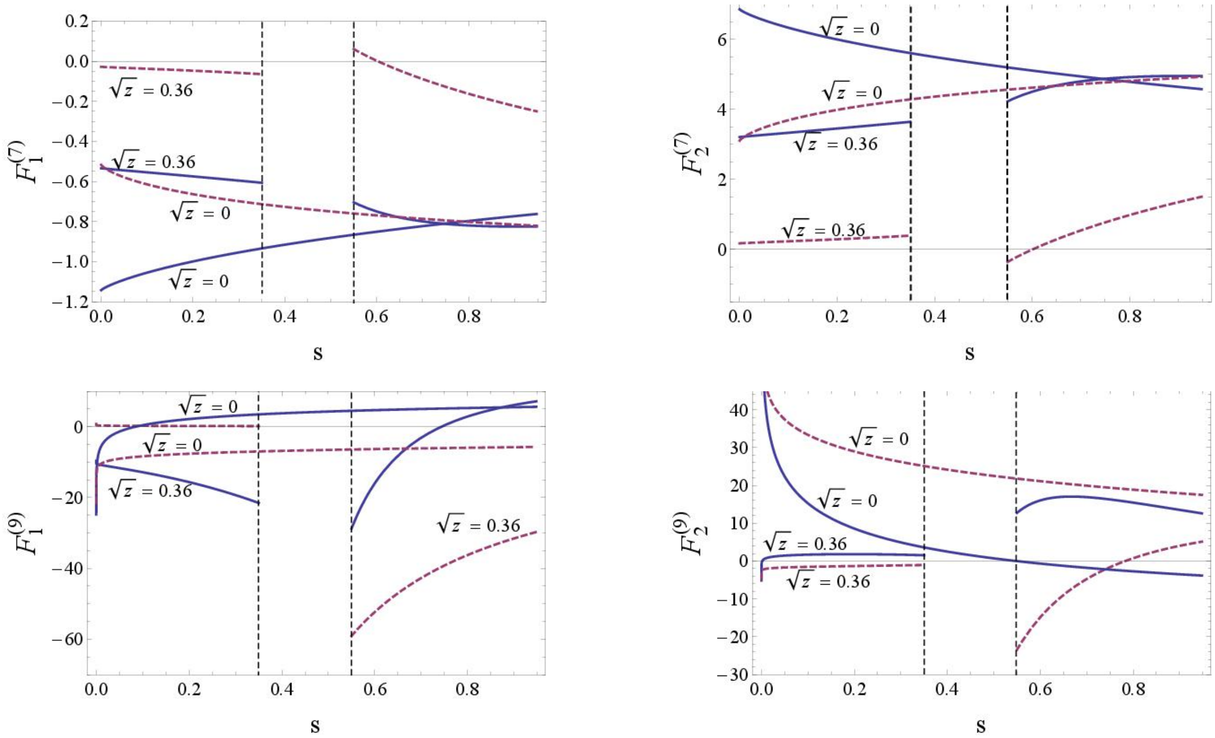

Figure 2: (Color online.) The real (solid lines) and imaginary parts (dotted lines) of the functions $F_{1,2}^{(7)}(s)$ (top two frames) and $F_{1,2}^{(9)}(s)$ (bottom two frames) at the scale $\mu = m_b$. For plotting the curves with $\sqrt{z} = 0$, the exact analytic expressions [41] were used. For non-zero values of $\sqrt{z}$, the analytic two-loop expressions obtained as double expansions in $\sqrt{z}$ and s [35,36] are used in plotting these functions in the region $s \leq 0.35$, whereas the expansions in $\sqrt{z}$ and $1 - s$ [42] are used in the range $0.55 < s < 1$. For these curves, we have fixed $\sqrt{z} = 0.36$.

is used [31] ($x = 4z/s$):

$$h(z,s) = -\frac{4}{9}\ln\frac{z}{\mu^2} + \frac{8}{27} + \frac{4}{9}x - \frac{2}{9}(2+x)\sqrt{|1-x|}\begin{cases}\ln\left|\dfrac{1+\sqrt{1-x}}{1-\sqrt{1-x}}\right| - i\pi, & \text{for } x < 1,\\ 2\arctan(1/\sqrt{1-x}), & \text{for } x > 1.\end{cases} \tag{30}$$

The renormalized α_s-corrections $F_{1,2}^{(7)}(s)$ and $F_{1,2}^{(9)}(s)$ to the $b \to s\,\ell^+\ell^-$ matrix element originated by the $\mathcal{O}_1$- and $\mathcal{O}_2$-operators from the effective Hamiltonian are known analytically both at small-q^2 [35, 36] and large-q^2 [42] domains of the lepton invariant mass squared as expansions in $\sqrt{z} = m_c/m_b$. Note that to obtain the invariant-mass spectrum and forward-backward symmetry in the inclusive $B \to X_s\ell^+\ell^-$ decays the $F_{1,2,8}^{(7)}(s)$ and $F_{1,2,8}^{(9)}(s)$ functions were expressed in terms of master integrals and evaluated numerically [43]. The functions $F_{1(2),u}^{(7)}(s)$ and $F_{1(2),u}^{(9)}(s)$ which are important in the $b \to d\,\ell^+\ell^-$ transitions were also calculated analytically first as an expansion in powers of s [38] and later exactly [41] from which the later expressions are used by us as we are considering the $B \to \pi \ell^+ \ell^-$ decay in the entire q^2-region.

The functions $F_{1,2}^{(7)}(s)$ (the top two frames) and $F_{1,2}^{(9)}(s)$ (the bottom two frames) are presented in Fig. 2 at the scale $\mu = m_b$ and $\sqrt{z} = 0.36$. The real and imaginary parts of these functions are shown by the solid and dashed lines, respectively. The functions $F_{1,2}^{(7)}(s)$ and $F_{1,2}^{(9)}(s)$ at $\sqrt{z} = 0$, which are obtained analytically in Ref. [41], are also shown in the same manner in Fig. 2. The vertical dashed lines specify the s-region where the expansions no longer hold. Note that this is also the interval in which charmonium resonances contribute. As the correct analytical functions in this region are not known for realistic value of $\sqrt{z}$, we have extrapolated the known analytic expressions (in the form of expansions in s and $1-s$) to the resonant region and found the matching value somewhere inside that the branching fraction has a minimal discontinuity This allow us to get a rough estimate of the differential branching fraction in the gap between the J/ψ- and $\psi(2S)$-resonances.

In the analysis we also used the renormalized α_s-corrections $F_8^{(7,9)}(s)$ from the $\mathcal{O}_8$-operator valid in the full kinematic q^2-domain ($0 \leq s \leq 1$) [42]:

$$
\begin{aligned}
F_8^{(7)}(s) &= \frac{4\pi^2}{27} \frac{2+s}{(1-s)^4} - \frac{4(11-16s+8s^2)}{9(1-s)^2} - \frac{8\sqrt{s(4-s)}}{9(1-s)^3} \left(9-5s+2s^2\right) \arcsin \frac{\sqrt{s}}{2} \\
&- \frac{16(2+s)}{3(1-s)^4} \arcsin^2 \frac{\sqrt{s}}{2} - \frac{8s \ln s}{9(1-s)} - \frac{8i\pi}{9} - \frac{32}{9} \ln \frac{\mu}{m_b}, \qquad (31) \\
F_8^{(9)}(s) &= -\frac{8\pi^2}{27} \frac{4-s}{(1-s)^4} + \frac{8(5-2s)}{9(1-s)^2} + \frac{16\sqrt{4-s}}{9\sqrt{s}\,(1-s)^3} \left(4+3s-s^2\right) \arcsin \frac{\sqrt{s}}{2} \\
&+ \frac{32(4-s)}{3(1-s)^4} \arcsin^2 \frac{\sqrt{s}}{2} + \frac{16 \ln s}{9(1-s)}, \qquad (32)
\end{aligned}
$$

where the mass m_b of the b-quarks is assumed to be the pole one.

To perform the numerical analysis one needs to know the $B \to \pi$ transition form factors $f_+(q^2)$, $f_0(q^2)$ and $f_T(q^2)$ in the entire kinematic range:

$$
4m_\ell^2 \leq q^2 \leq (m_B - m_\pi)^2 . \qquad (33)
$$

Their model-independent determination is the main aim of this paper, which is described in detail in subsequent sections.

3 Form-Factor Parametrizations

Several parametrizations of the semileptonic form factors $f_+(q^2)$, $f_0(q^2)$ and $f_T(q^2)$ have been proposed in the literature. The four parametrizations of $f_+(q^2)$ discussed below have been used in the analysis of the semileptonic data on $B \to \pi \ell \nu_\ell$. All of them include at least one pole term at $q^2 = m_{B^*}^2$, where $m_{B^*} = 5.325$ GeV [26] is the vector B^*-meson mass. As far as this mass satisfies the condition $m_{B^*} < m_B + m_\pi$, i.e., it lies below the so-called continuum threshold, it should be included into the form factor as a separate pole. Mesons and multi-particle states with the appropriate $J^P = 1^-$ quantum number can be described either by one or several poles or by some other rapidly convergent function, both effectively counting the continuum. The tensor form factor $f_T(q^2)$ shows a similar qualitative behavior and its model function obeys the same shape as the vector one. The case of the scalar form factor $f_0(q^2)$ is different as the first orbitally-excited scalar B^{**}-meson with $J^P = 0^+$ (it is expected to be somewhere within the signal called as the $B_J^*(5732)$ resonance [26] with the mass $m_{B_J^*(5732)} = 5698 \pm 8$ MeV and width $\Gamma_{B_J^*(5732)} = 128 \pm 18$ MeV which can be interpreted as stemming from several narrow and broad resonances[5]) has the mass squared above the continuum threshold $t_0 = (m_B + m_\pi)^2 = 29.36$ GeV^2 and, hence, it belongs to the continuum which makes $f_0(q^2)$ regular at $q^2 = m_{B^*}^2$, in contrast to $f_+(q^2)$ and $f_T(q^2)$.

3.1 The Becirevic-Kaidalov Parametrization

The form factor $f_+(q^2)$ in the Becirevic-Kaidalov (BK) parametrization [12] can be written as follows:

$$f_+(q^2) = \frac{f_+(0)}{(1 - \hat{q}_*^2)\,(1 - \alpha_{\rm BK}\,\hat{q}_*^2)}, \tag{34}$$

where $\hat{q}_*^2 = q^2/m_{B^*}^2$. The fitted parameters are the form-factor normalization, $f_+(0)$, and $\alpha_{\rm BK}$ which defines the $f_+(q^2)$ shape [12]. This parametrization is one of the simplest ones. The shape of the tensor form factor $f_T(q^2)$ is the same (34) as it also has the pole at $q^2 = m_{B^*}^2$ below the continuum threshold. The scalar form factor $f_0(q^2)$ was also introduced in its simplest form [12]:

$$f_0(q^2) = \frac{f_+(0)}{1 - \hat{q}_*^2/\beta_{\rm BK}}, \tag{35}$$

with the same normalization factor $f_+(0)$ but a different effective pole position determined by the free parameter $\beta_{\rm BK}$.

This form-factor parametrizations should be taken with caution, since the simple two-parameter shape is overly restrictive and has been argued to be inconsistent with the requirements from the Soft-Collinear Effective Theory (SCET) [15].

3.2 The Ball-Zwicky Parametrization

The Ball-Zwicky (BZ) parametrization for the vector form factor $f_+(q^2)$ is a modified form of the BK parametrization, given as [6]:

$$f_+(q^2) = \frac{f_+(0)}{1 - \hat{q}_*^2}\left[1 + \frac{r_{\rm BZ}\,\hat{q}_*^2}{1 - \alpha_{\rm BZ}\,\hat{q}_*^2}\right] = \frac{f_+(0)\,[1 - (\alpha_{\rm BZ} - r_{\rm BZ})\,\hat{q}_*^2]}{(1 - \hat{q}_*^2)\,(1 - \alpha_{\rm BZ}\hat{q}_*^2)}, \tag{36}$$

where the fitted parameters are $f_+(0)$, $\alpha_{\rm BZ}$, and $r_{\rm BZ}$. $f_+(0)$ sets again the normalization of the form factor, while $\alpha_{\rm BZ}$ and $r_{\rm BZ}$ define the shape [6]. In particular, for $\alpha_{\rm BZ} = r_{\rm BZ}$

[5] Approximately the same mass difference $m_{B_s^{**}} - m_{B_s} = 385 \pm 16 \pm 5 \pm 25$ MeV in the B_s-meson sector was obtained by the HPQCD Collaboration [44].

one reproduces the BK parametrization (34). The same redefinition is also applied to the tensor form factor $f_T(q^2)$. In a similar way the scalar form factor $f_0(q^2)$ (35) can be modified by introducing its own second free parameter $r_{\rm BZ}^{(0)}$.

3.3 The Boyd-Grinstein-Lebed Parametrization

This parametrization was introduced for the form factors entering both the heavy-to-light [13] and heavy-to-heavy [45] transition matrix elements and used in the analysis of the semileptonic $B \to D^{(*)}\ell\nu_\ell$ [45–47] and $B \to \pi\ell\nu_\ell$ [13, 48] decays. The basic idea is to find an appropriate function $z(q^2, q_0^2)$ in term of which the form factor can be written as a Taylor series with good convergence for all physical values of q^2 so that the form factor can be well described by the first few terms in the expansion. The generalization of this parametrization to additional form factors entering rare semileptonic $B \to h_L\,\ell^+\ell^-$, where h_L is the pseudoscalar K- or the vector ρ- or K^*-mesons, and $B_s \to \phi\,\ell^+\ell^-$ decays, was undertaken in [49]. As this will be our default parametrization in our analysis, we discuss it at some length.

The following shape for the form factors $f_i(q^2)$ with $i = +, 0, T$ is suggested in the BGL parametrization [13]:

$$f_i(q^2) = \frac{1}{P(q^2)\phi_i(q^2, q_0^2)} \sum_{k=0}^{k_{\rm max}} a_k(q_0^2) \left[z(q^2, q_0^2)\right]^k, \tag{37}$$

where the following form for the function $z(q^2, q_0^2)$ is used:

$$z(q^2, q_0^2) = \frac{\sqrt{m_+^2 - q^2} - \sqrt{m_+^2 - q_0^2}}{\sqrt{m_+^2 - q^2} + \sqrt{m_+^2 - q_0^2}}, \tag{38}$$

with the pair-production threshold $m_+^2 = (m_B + m_\pi)^2$ and a free parameter q_0^2. The function $z(q^2, q_0^2)$ maps the entire range of q^2 onto the unit disc $|z| \leq 1$ in a way that the minimal physical value $z_{\rm min} = z(m_-^2, q_0^2)$ corresponds to the lowest hadronic recoil $q_{\rm max}^2 = m_-^2 = (m_B - m_\pi)^2$, the maximal value $z_{\rm max}$ is reached at $q^2 = 0$, and $z(q^2, q_0^2)$ vanishes at $q^2 = q_0^2$. In early studies of the form factors, the parameter q_0^2 was often taken to be $q_0^2 = m_-^2$ [13, 45], so that $z_{\rm min} = 0$. In this case, the maximal value $z_{\rm max} = 0.52$ for the $B \to \pi\ell\nu_\ell$ decay is not small but enough to constrain the form factor $f_+(q^2)$ [48, 50]. To decrease the value of $z_{\rm max}$, and improve the convergence of the Taylor series in (37), it was proposed to take a smaller (optimal) value of q_0^2 somewhere in the interval $0 < q_0^2 < m_-^2$ [51]. In our analysis we make the choice $q_0^2 = 0.65 m_-^2$ following [8], so that $-0.34 < z(q^2, q_0^2) < 0.22$ in the entire range $0 < q^2 < m_-^2$.

The proposed shape (37) for the form factor contains the so-called Blaschke factor $P(q^2)$ which accounts for the hadronic resonances in the sub-threshold region $q^2 < m_+^2$. For the semileptonic $B \to \pi\ell\nu_\ell$ decay, where ℓ is an electron or a muon, there is only B^*-meson with the mass $m_{B^*} = 5.325$ GeV satisfying the sub-threshold condition and producing the pole in the form factor at $q^2 = m_{B^*}^2$. In this case, the Blaschke factor is simply $P(q^2) = z(q^2, m_{B^*}^2)$ for $f_{+,T}(q^2)$ and $P(q^2) = 1$ for $f_0(q^2)$.

Table 2: Parameters entering the outer functions $\phi_i(q^2, q_0^2)$ defined in (40) with $i = +, 0, T$ in the $B \to \pi$ transition form factors.

f_i	K_i	α_i	β_i	$\chi_i^{(0)}$
f_+	48π	3	2	7.005×10^{-4} GeV^{-2}
f_0	$16\pi/(m_+^2 m_-^2)$	1	1	1.452×10^{-2}
f_T	$48\pi m_+^2$	3	1	1.811×10^{-3} GeV^{-2}

The coefficients a_k ($k = 0, 1, \ldots, k_{\rm max}$) entering the Taylor series in Eq. (37) are the parameters, which are determined by fits of the data. The outer function $\phi_i(q^2, q_0^2)$ is an arbitrary analytic function, whose choice only affects particular values of the coefficients a_k and allows one to get a simple constraint from the dispersive bound [48][6]:

$$\sum_{k=0}^{\infty} a_k^2 \leq 1. \tag{39}$$

This restriction can be achieved with the following outer function [52]:

$$\begin{aligned} \phi_i(q^2, q_0^2) \;&=\; \sqrt{\frac{n_I}{K_i \chi_{f_i}^{(0)}}} \left(\sqrt{m_+^2 - q^2} + \sqrt{m_+^2 - q_0^2}\right) \frac{(m_+^2 - q^2)^{(\alpha_i+1)/4}}{(m_+^2 - q_0^2)^{1/4}} \\ &\times \left(\sqrt{m_+^2 - q^2} + \sqrt{m_+^2 - m_-^2}\right)^{\alpha_i/2} \left(\sqrt{m_+^2 - q^2} + m_+\right)^{-(3+\beta_i)}, \end{aligned} \tag{40}$$

where $n_I = 3/2$ is the isospin factor, while the values of K_i, α_i and β_i are collected in Table 2. The numerical quantities $\chi_{f_i}^{(0)}$ are obtained from the derivatives of the scalar functions entering the corresponding correlators calculated by the operator product expansion method [48, 49, 51]. In the two-loop order at the mass scale μ_b they are as follows [49]:

$$\chi_{f_+}^{(0)} = \frac{3}{32\pi^2 m_b^2}\left(1 + \frac{C_F \alpha_s(\mu_b)}{4\pi}\,\frac{25 + 4\pi^2}{6}\right) - \frac{\langle\bar{q}q\rangle}{m_b^5} - \frac{\langle\alpha_s G^2\rangle}{12\pi m_b^6} + \frac{3\langle\bar{q}Gq\rangle}{m_b^7}, \tag{41}$$

$$\chi_{f_0}^{(0)} = \frac{1}{8\pi^2}\left(1 + \frac{C_F \alpha_s(\mu_b)}{4\pi}\,\frac{3 + 4\pi^2}{6}\right) + \frac{\langle\bar{q}q\rangle}{m_b^3} + \frac{\langle\alpha_s G^2\rangle}{12\pi m_b^4} - \frac{3\langle\bar{q}Gq\rangle}{2m_b^5}, \tag{42}$$

$$\chi_{f_T}^{(0)} = \frac{1}{4\pi^2 m_b^2}\left(1 + \frac{C_F \alpha_s(\mu_b)}{4\pi}\left[\frac{10 + 2\pi^2}{3} + 8\ln\frac{m_b}{\mu_b}\right]\right) - \frac{\langle\bar{q}q\rangle}{m_b^5} - \frac{\langle\alpha_s G^2\rangle}{24\pi m_b^6} + \frac{7\langle\bar{q}Gq\rangle}{2m_b^7}, \tag{43}$$

where $C_F = 4/3$, and m_b is the mass of the b-quark in the loops which is identified with the $\overline{\rm MS}$ b-quark mass $\bar{m}_b(\bar{m}_b) = 4.18$ GeV [26]. For the evaluation of $\chi_{f_i}^{(0)}$ it is enough to use the central values of the input parameters to get the overall numerical normalization factor for the form factors and the existing uncertainties in $\chi_{f_i}^{(0)}$ are of not much consequence. The following input values are used: $\alpha_s(M_Z) = 0.1184 \pm 0.0007$ [26], $\langle\bar{q}q\rangle(1~\text{GeV}) = -(1.65 \pm$

[6] The definition for $f_0(q^2)$ in accordance with Ref. [49] results in even stronger bound $\sum_{k=0}^{\infty} a_k^2 \leq 1/3$.

$0.15) \times 10^{-2}$ GeV^3, $\langle \bar{q}Gq \rangle = \langle \bar{q} g_s \sigma^{\mu\nu} G^A_{\mu\nu} T^A q \rangle = m_0^2 \langle \bar{q}q \rangle$, $m_0^2(1 \text{ GeV}) = 0.8 \pm 0.2$ GeV^2, and $\langle (\alpha_s/\pi)\, G^2 \rangle = 0.005 \pm 0.004$ GeV^4 from Ref. [53]. While the mixed quark-gluon $\langle \bar{q}Gq \rangle$ and the two-gluon $\langle (\alpha_s/\pi)\, G^2 \rangle$ condensates are practically scale-independent quantities [53], the strong coupling and the quark condensate have to be evolved to the scale of the b-quark mass where they have the values $\alpha_s(\bar{m}_b) = 0.227$ to the two-loop accuracy and $\langle \bar{q}q \rangle(\bar{m}_b) = -0.023$ GeV^3. Numerical values of $\chi^{(0)}_{f_i}$ are presented in Table 2. They agree well (up to 5%) with the ones presented in Table 2 of [49], despite difference in the input parameters. Note that the BaBar collaboration [8] used approximately the same value $\chi^{(0)}_{f_+} = 6.889 \times 10^{-4}$ GeV^{-2} in the analysis of the $B^0 \to \pi^+ \ell^- \nu_\ell$ decays.

Having relatively small values of $z(q^2, q_0^2)$ in the physical region of q^2, the shape of the form factor can be well approximated by the truncated series at $k_{\rm max} = 2$ or 3 [46].

3.4 The Bourrely-Caprini-Lellouch Parametrization

The problems with the from-factor asymptotic behavior at $|q^2| \to \infty$ and truncation of the Taylor series found in the BGL-parametrization [14,15] were solved by the introduction of another representation of the series expansion (called the Simplified Series Expansion — SSE [49]). The shape suggested for the vector $f_+(q^2)$ form factor [14] was extended to the other two, scalar $f_0(q^2)$ and tensor $f_T(q^2)$ form factors [49]:

$$f_+(q^2) = \frac{1}{1-\hat{q}_*^2} \sum_{k=0}^{k_{\rm max}} b_k(q_0^2) \left[z(q^2, q_0^2) \right]^k , \tag{44}$$

$$f_0(q^2) = \frac{m_B^2}{m_B^2 - m_\pi^2} \sum_{k=0}^{k_{\rm max}} b_k(q_0^2) \left[z(q^2, q_0^2) \right]^k , \tag{45}$$

$$f_T(q^2) = \frac{m_B + m_\pi}{m_B\,(1-\hat{q}_*^2)} \sum_{k=0}^{k_{\rm max}} b_k(q_0^2) \left[z(q^2, q_0^2) \right]^k , \tag{46}$$

where $\hat{q}_*^2 = q^2/m_{B^*}^2$ and the function $z(q^2, q_0^2)$ is defined in Eq. (38). In this expansion the shape of the form factor is determined by the values of b_k, with truncation at $k_{\rm max} = 2$ or 3. The value of the free parameter q_0^2 is proposed to be the so-called optimal one $q_0^2 = q^2_{\rm opt} = (m_B + m_\pi) \left(\sqrt{m_B} - \sqrt{m_\pi} \right)^2$ [14] which is obtained as the solution of the equation $z(0, q_0^2) = -z(m_-^2, q_0^2)$ (the latter condition means that the physical range $0 < q^2 \leq m_-^2$ is projected onto a symmetric interval on the real axis in the complex z-plane). The prefactors $1/(1-\hat{q}_*^2)$ in $f_+(q^2)$ and $f_T(q^2)$ allow one to get the right asymptotic behavior $\sim 1/q^2$ predicted by the perturbative QCD. In Ref. [14, 15] an additional restriction on the series coefficients was discussed. In particular, in the case of $f_+(q^2)$ at $q^2 \sim m_+^2$, the threshold behavior of the form factor results in a constraint on its derivative, $df_+/dz|_{z=-1} = 0$ [14], which allows one to eliminate the last term in the truncated expansion as follows:

$$b_{k_{\rm max}} = -\frac{(-1)^{k_{\rm max}}}{k_{\rm max}} \sum_{k=0}^{k_{\rm max}-1} (-1)^k\, k\, b_k. \tag{47}$$

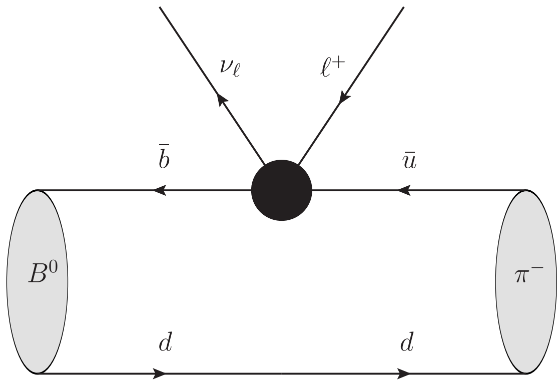

Figure 3: Feynman diagram for the decay $B^0 \to \pi^- \ell^+ \nu_\ell$.

In the case of $f_0(q^2)$ the threshold behavior is different and a similar relation is not applied. To the best of our knowledge, a detailed analysis of the additional constraints based on the threshold behavior of the tensor $f_T(q^2)$ form factor has not yet been performed. This behavior, however, is not expected to be very different from the one found for the vector $f_+(q^2)$ form factor. So, one may as well put the condition on the derivative $df_T/dz|_{z=-1} = 0$ in this case, which allows to eliminate the last term in the truncated expansion for $f_T(q^2)$.

4 Extraction of the $f_+(q^2)$ Form-Factor Shape

4.1 The $B^0 \to \pi^- \ell^+ \nu_\ell$ Branching Fraction

The charged-current Lagrangian inducing the $b \to u$ transition in the SM is:

$$\mathcal{L}_W(x) = -\frac{g}{2\sqrt{2}} V_{ub} \left[\bar{u}(x)\gamma_\mu (1-\gamma_5) b(x)\right] W^\mu(x) + \text{h. c.}, \tag{48}$$

where g is the $SU(2)_L$ coupling, V_{ub} is the element of the CKM matrix, $u(x)$ and $b(x)$ are the u- and b-quark fields, and $W(x)$ is the W-boson field. Feynman diagram for the $B^0 \to \pi^- \ell^+ \nu_\ell$ decay is shown in Fig. 3 and the one for the $B^+ \to \pi^0 \ell^+ \nu_\ell$ decay differs by the exchange of the spectator-quark flavor ($d \to u$) only. The $B \to \pi$ transition matrix element entering the B-meson decay $B \to \pi \ell \nu_\ell$, can be parametrized in terms of two form factors $f_+(q^2)$ and $f_0(q^2)$ as follows [54, 55]:

$$\langle \pi(p_\pi)|\bar{u}\gamma^\mu b|B(p_B)\rangle = f_+(q^2)\left[p_B^\mu + p_\pi^\mu - \frac{m_B^2 - m_\pi^2}{q^2}\, q^\mu\right] + f_0(q^2)\,\frac{m_B^2 - m_\pi^2}{q^2}\, q^\mu. \tag{49}$$

Here, p_B (m_B) and p_π (m_π) are the four-momenta (masses) of the B- and π-mesons, respectively. In the isospin-symmetry limit, the form factors entering in the charged-current matrix element (49) are exactly the same as the ones in Eq. (15) in the FCNC process $B \to \pi\, \ell^+ \ell^-$.

Measurements of the $B^0 \to \pi^- \ell^+ \nu_\ell$ and $B^+ \to \pi^0 \ell^+ \nu_\ell$ decays, where $\ell = e$, μ, allow to extract both the CKM matrix element $|V_{ub}|$ and the shape of the $f_+(q^2)$ form factor. The differential branching fractions of the above processes can be written in the form [26]:

$$\frac{d\Gamma(B \to \pi \ell^+ \nu_\ell)}{dq^2} = C_P \, \frac{G_F^2 |V_{ub}|^2}{192 \pi^3 m_B^3} \, \lambda^{3/2}(q^2) f_+^2(q^2) \tag{50}$$

where G_F is the Fermi constant, C_P is the isospin factor with $C_P = 1$ for the π^+-meson and $C_P = 1/2$ for the π^0-meson, $\lambda(q^2)$ is the standard three-body kinematic factor (18), $q = p_\ell + p_\nu$ is the total four-momentum transfer, bounded by $m_\ell^2 \leq q^2 \leq (m_B - m_\pi)^2$, and p_ℓ and p_ν are the four-momenta of the charged lepton and the neutrino, respectively. In general, the $B \to \pi$ transition matrix element (49) depends on two form factors, in practice, however, only $f_+(q^2)$ is measurable in the $B \to \pi \ell \nu_\ell$ decays with electrons and muons, since the contribution of the scalar form factor $f_0(q^2)$ to the decay rate is suppressed by the mass ratio of the charged lepton to the B-meson [55].

The values of G_F, m_B, and m_π are known with high accuracy [26], while the experimentally derived value of $|V_{ub}|$ depends somewhat on the extraction method and B-meson decays considered. This is discussed at great length in the Particle Data Group (PDG) reviews [26]. The value quoted from the analysis of the exclusive $B \to \pi \ell \bar{\nu}$ decay is listed there as $|V_{ub}| = (3.23 \pm 0.31) \times 10^{-3}$. On the other hand, assuming the SM, the CKM unitarity fits yield a value of $|V_{ub}|$ which is consistent with the previous value, but it is about a factor 2 more precise [26]: $|V_{ub}| = (3.51^{+0.15}_{-0.14}) \times 10^{-3}$, which we use as our default value in the numerical estimates.

The partial branching fractions for the $B^0 \to \pi^- \ell^+ \nu_\ell$ decays has been measured by the CLEO, BaBar and Belle collaborations, and for the $B^+ \to \pi^0 \ell^+ \nu_\ell$ decays by the Belle collaboration. Below we give the total branching fraction of the $B^0 \to \pi^- \ell^+ \nu_\ell$ decay taking into account the recent data from the BaBar and Belle collaborations [10,11,56,57]:

$$\mathcal{B}(B^0 \to \pi^- \ell^+ \nu_\ell) = \begin{cases} (1.42 \pm 0.05_{\rm stat} \pm 0.07_{\rm syst}) \times 10^{-4} & [\text{BaBar, 2011}]\ , \\ (1.45 \pm 0.04_{\rm stat} \pm 0.06_{\rm syst}) \times 10^{-4} & [\text{BaBar, 2012}]\ , \\ (1.49 \pm 0.04_{\rm stat} \pm 0.07_{\rm syst}) \times 10^{-4} & [\text{Belle, 2011}]\ , \\ (1.49 \pm 0.09_{\rm stat} \pm 0.07_{\rm syst}) \times 10^{-4} & [\text{Belle, 2013}]\ . \end{cases} \tag{51}$$

All these measurements are in excellent agreement with each other, and with the one for the $B^+ \to \pi^0 \ell^+ \nu_\ell$ decay reported by the Belle collaboration [11]:

$$\mathcal{B}(B^+ \to \pi^0 \ell^+ \nu_\ell) = (0.80 \pm 0.08_{\rm stat} \pm 0.04_{\rm syst}) \times 10^{-4}. \tag{52}$$

Both the collaborations have presented differential distributions in q^2 relevant for the extraction of $f_+(q^2)$ from data [10, 11, 56, 57]. We show them in the next subsection, where also our fitting procedure is presented.

4.2 Fitting Procedure

In this subsection the extraction of the $f_+(q^2)$ form-factor shape from the dilepton invariant-mass spectra in the $B^0 \to \pi^- \ell^+ \nu_\ell$ and $B^+ \to \pi^0 \ell^+ \nu_\ell$ decays measured by the BaBar [56,57]

Table 3: Summary of the $\chi^2_{\rm min}$/ndf values, where ndf is the number of degrees of freedom, (corresponding p-values) for different sets of experimental data (rows) and different form-factor parametrizations (columns).

	BK [12]	BZ [6]	BGL [46]	BCL [14]
BaBar 2011 [56]	9.93/10 (45%)	4.80/9 (85%)	4.12/9 (90%)	3.75/9 (93%)
BaBar 2012 [57]	8.68/10 (56%)	5.50/9 (79%)	5.65/9 (77%)	5.73/9 (77%)
Belle 2011 [10]	15.86/11 (15%)	14.55/10 (15%)	12.97/10 (23%)	14.44/10 (15%)
Belle 2013 [11]	24.41/18 (14%)	23.55/17 (13%)	24.16/17 (12%)	23.26/17 (14%)
BaBar & Belle	44.99/43 (39%)	44.91/42 (35%)	44.56/42 (36%)	44.77/42 (36%)

and Belle [10,11] collaborations is explained. All four $f_+(q^2)$ form-factor parametrizations from Sec. 3 are examined to test their consistency with the experiment in terms of the best-fit values resulting from the χ^2-distribution function [26].

The fitted form factor is presented as a function of q^2 which contains a set of k unknown parameters $\alpha_1, \ldots, \alpha_k$:

$$f_+(q^2) = f(q^2; \alpha_1, \ldots, \alpha_k). \tag{53}$$

Given the experimental values y_i of the partial branching fractions $\Delta\mathcal{B}(q^2)/\Delta q^2$ in bins of q^2, with their uncertainties σ_i, the χ^2-distribution function is defined as follows [26]:

$$\chi^2 = \sum_{i=1}^{N} \frac{\left(y_i - F(x_i; \alpha_1, \ldots, \alpha_k)\right)^2}{\sigma_i^2}, \tag{54}$$

where N is the number of experimental points and $F(x_i; \alpha_1, \ldots, \alpha_k)$ denotes the theoretical estimates of the partial branching fractions $\Delta\mathcal{B}(q^2)/\Delta q^2$ for the given parametrization:

$$F(x_i; \alpha_1, \ldots, \alpha_k) = \int\limits_{x_i - a_i/2}^{x_i + a_i/2} \frac{d\mathcal{B}(q^2)}{dq^2}\, dq^2, \tag{55}$$

with x_i and a_i being the center and the width of the ith bin. The standard minimization procedure of the χ^2-function (minimum of this function is denoted as $\chi^2_{\rm min}$) allows us to extract the values of fitted parameters $\alpha_{1,\rm min}, \ldots, \alpha_{k,\rm min}$, which are considered to be their best-fit values. The results obtained by using the four form-factor parametrizations for different sets of experimental data obtained by the BaBar [56, 57] and Belle [10, 11] collaborations are presented in Figs. 4 and 5, respectively, and the numerical values for $\chi^2_{\rm min}$/ndf, where ndf is the number of degrees of freedom, and the corresponding p-values are presented in Table 3. The results from the combined analysis of the BaBar and Belle data sets are shown in Fig. 6. In this analysis we have assumed that the experimental points are all uncorrelated.

From Table 3 it follows that the smallest value for $\chi^2_{\rm min}$/ndf corresponds to the simplest Becirevic-Kaidalov parametrization. From the rest of the specified parametrizations, the

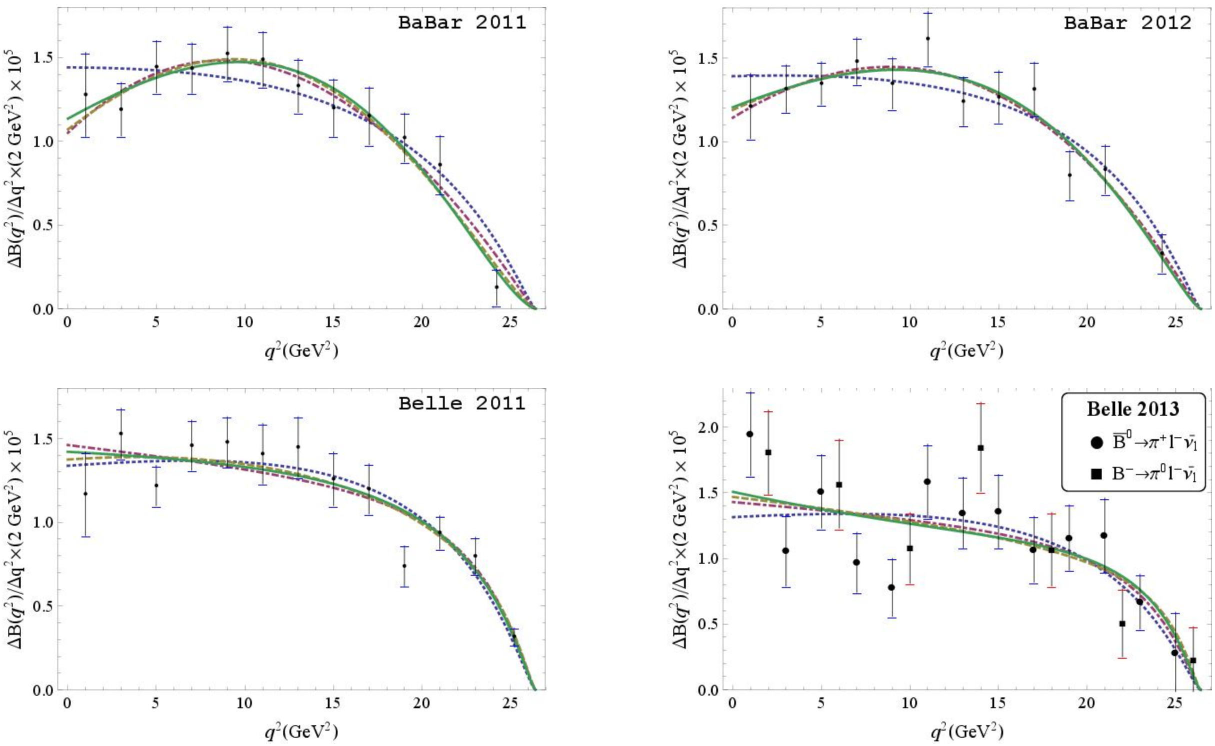

Figure 4: (Color online.) Partial $\Delta\mathrm{Br}(q^2)/\Delta q^2$ spectra for the $B^0 \to \pi^- \ell^+ \nu_\ell$ and $B^+ \to \pi^0 \ell^+ \nu_\ell$ decays, where $\ell = e,\, \mu$. The data points (black dots) are placed in the middle of each bin. The error bars (blue) include the total experimental uncertainties. The curves show the results of the fit to the data for the four form-factor parametrizations discussed in the text: BK (34) (thick dotted blue line), BZ (36) (thick dashed purple line), BGL (37) with $k_{\max} = 2$ (thick dot-dashed yellow line), and BCL (44) with $k_{\max} = 2$ (thick solid green line). The upper-left and upper-right plots correspond to the BaBar 2011 [56] and 2012 [57] data sets, while the lower-left and lower-right plots are plotted based on the Belle 2011 [10] and 2013 [11] data sets.

Boyd-Grinstein-Lebed one has the smallest $\chi^2_{\min}/\mathrm{ndf}$ value and we will use it for all the form factors entering the $B \to \pi \ell^+ \ell^-$ decay.

The combined analysis of the BaBar and Belle data results the following set of fitted parameters entering the $f_+(q^2)$ form factor expansion in the BGL parametrization truncated at $k_{\max} = 2$:

$$\begin{aligned} a_0 &= 0.0209 \pm 0.0004, \\ a_1 &= -0.0306 \pm 0.0031, \\ a_2 &= -0.0473 \pm 0.0189. \end{aligned} \tag{56}$$

The numerical values extracted depend on the CKM matrix element $|V_{ub}|$ and correspond to the PDG value [26]: $|V_{ub}| = (3.51^{+0.15}_{-0.14}) \times 10^{-3}$. The errors specified in the coefficients (56) are the square roots of the covariance matrix U_{ij} for the BGL form-factor

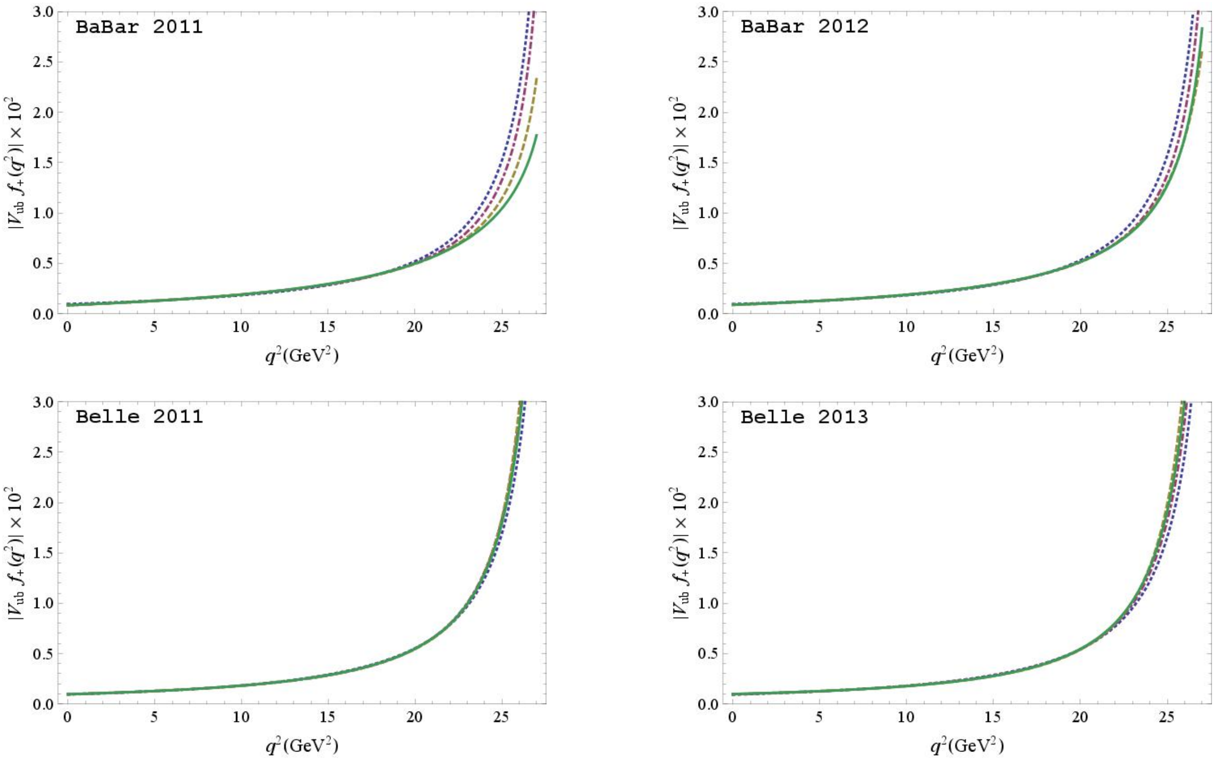

Figure 5: (Color online.) The $f_+(q^2)$ form-factor shapes multiplied by the CKM matrix element $|V_{ub}|$ following from the BaBar [56, 57] and Belle [10, 11] data. The curves show the results of the fit to these data: BK (34) (thick dotted blue line), BZ (36) (thick dashed purple line), BGL (37) with $k_{\max} = 2$ (thick dot-dashed yellow line), and BCL (44) with $k_{\max} = 2$ (thick solid green line) parametrizations.

coefficients which can be derived from the χ^2-function (54) as follows [26]:

$$\left(U^{-1}\right)_{ij} = \frac{1}{2}\, \frac{\partial^2 \chi^2}{\partial \alpha_i \partial \alpha_j}\bigg|_{\alpha_k = \hat{\alpha}_k}, \tag{57}$$

where $\hat{\alpha}_k$ are the best-fit values of the fitting parameters. The BGL form factor belongs to the case for which the function $F(x_i; \alpha_1, \ldots, \alpha_k)$ depends linearly on the unknown parameters, which simplifies the analysis. The corresponding correlation matrix r_{ij} is connected with the covariance matrix by the relation $r_{ij} = U_{ij}/(\sigma_i\, \sigma_j)$, where σ_i^2 is the variance of α_i. For the BGL form factor with the truncation at $k_{\max} = 2$, the following (3×3) correlation matrix was obtained:

$$r_{ij} = \begin{pmatrix} 1 & -0.26 & -0.43 \\ -0.26 & 1 & -0.68 \\ -0.43 & -0.68 & 1 \end{pmatrix}. \tag{58}$$

One can see a strong correlation of the third coefficient a_2 in the z-expansion with the other two a_0 and a_1. This is shown in Fig. 7. The relative error on the coefficient a_2 is approximately 40% as ca also be seen in Eq. (56)

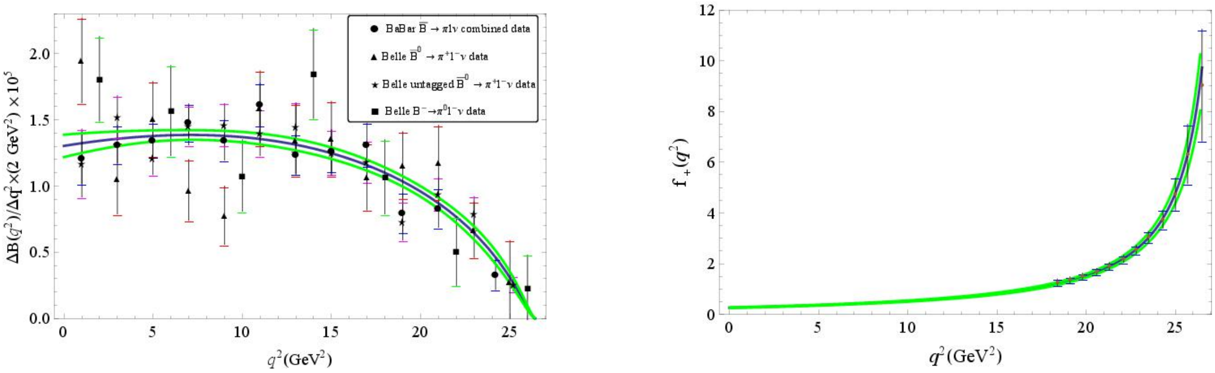

Figure 6: (Color online.) Partial $\Delta\mathcal{B}(q^2)/\Delta q^2$ spectra for the decays $B^0 \to \pi^- \ell^+ \nu_\ell$ and $B^+ \to \pi^0 \ell^+ \nu_\ell$ are presented on the left plot. The $f_+(q^2)$ form factor is shown on the right plot. The BGL parametrization is adopted as the preferred choice. Results are obtained by combining the experimental data by the BaBar [57] and Belle [10,11] collaborations and, in addition, the value $|V_{ub}| = (3.51^{+0.15}_{-0.14}) \times 10^{-3}$ [26]) is used to extract explicitly the form-factor shape. The existing Lattice-QCD data [58] on the form factor are presented as the vertical bars on the right plot.

5 Determination of $f_0(q^2)$ and $f_T(q^2)$ Shapes

As pointed out earlier, the form factor $f_0(q^2)$ is not required for either the charged-current decay $B \to \pi \ell \nu_\ell$ or the FCNC semileptonic $B \to \pi \ell^+ \ell^-$ decay with $\ell = e, \mu$, as its contribution to the branching fraction is suppressed by the smallness of the lepton mass squared. However, for the sake of completeness involving the semileptonic processes with $\ell^\pm = \tau^\pm$, we also work out the $f_0(q^2)$ form factor. The information on the form factors $f_+(q^2)$ and $f_0(q^2)$ for the $B \to \pi$ and $B \to K$ transitions is available, though the lattice results on the $B \to \pi$ form factor $f_T(q^2)$ are still scant. For our analysis, we use an Ansatz for the $SU(3)_F$-symmetry breaking to obtain the shape of $f_T^{B\pi}(q^2)$, from the corresponding $B \to K$ form factor $f_T^{BK}(q^2)$. We show subsequently that our Ansatz, which assumes that the $SU(3)_F$-symmetry breaking in $f_T(q^2)$ is an average of the corresponding symmetry-breaking effects in the form factors $f_+(q^2)$ and $f_0(q^2)$, yields an $f_T^{B\pi}(q^2)$, which is in good agreement with the preliminary results on this form factor, obtained from lattice in the low-recoil region.

5.1 The $f_0(q^2)$ Form Factor

The parameters of $f_0(q^2)$ can be obtained from the existing results of the $B \to \pi$ transition form factor calculated by the HPQCD collaboration [58]. In addition one can use the exact relation between $f_+(q^2)$ and $f_0(q^2)$ at $q^2 = 0$:

$$f_+(0) = f_0(0), \tag{59}$$

which follows from the requirement of the finiteness of the $B \to \pi$ transition matrix element (15) at this point. To fix $f_0(0)$, we use the reference point $f_+(0) = 0.261 \pm 0.014$, extracted by us from the experimental data. The form-factor parametrization we use

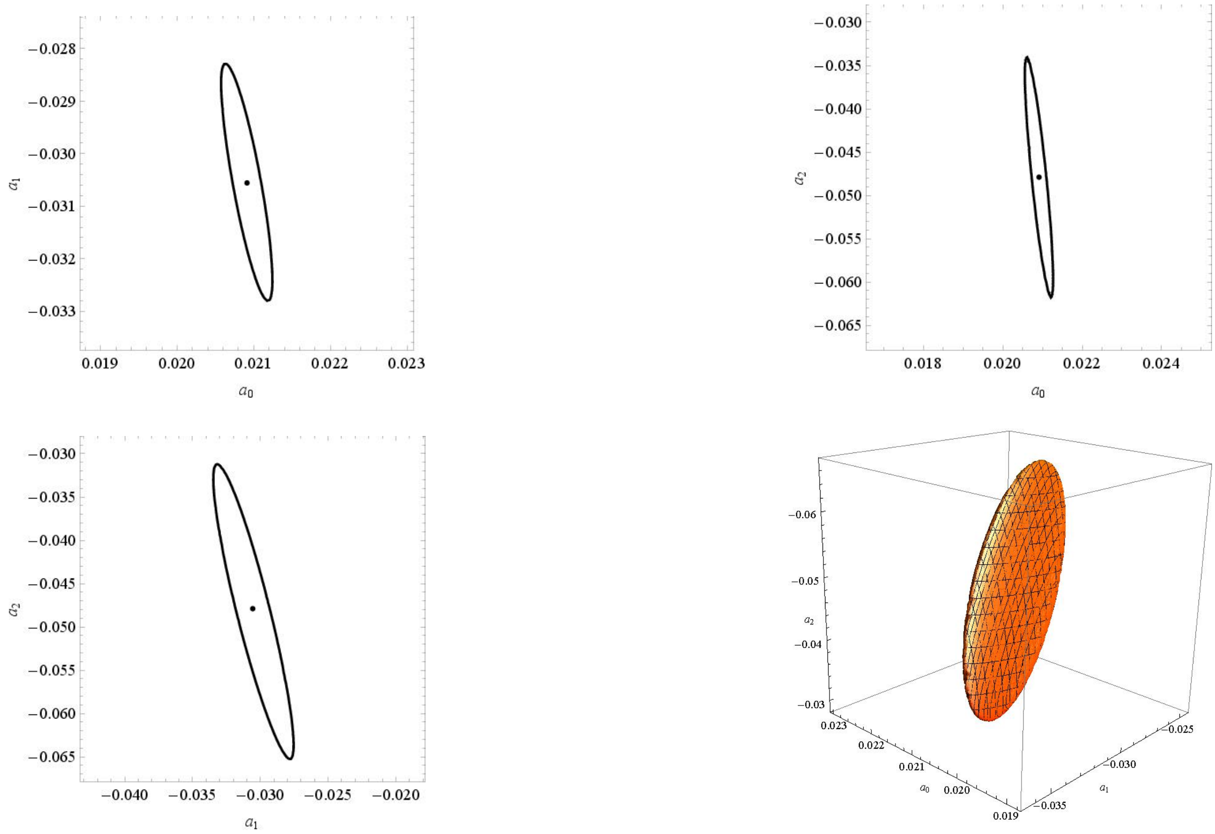

Figure 7: (Color online.) The two-dimensional correlations among the fitted parameters a_0, a_1 and a_2 entering the BGL-parametrization of the form factor $f_+(q^2)$: $a_0 - a_1$ (upper-left plot), $a_0 - a_2$ (upper-right plot) and $a_1 - a_2$ (lower-left plot). The three-dimensional correlation among all three fitted parameters is shown in the lower-right plot.

for $f_0(q^2)$ follows our default choice from the analysis of $f_+(q^2)$ — the BGL expansion in $z(q^2, q_0^2)$ truncated at $k_{\max} = 2$. The set of the fitted parameters entering $f_0(q^2)$ is as follows:

$$\begin{aligned} a_0 &= 0.0201 \pm 0.0007, \\ a_1 &= -0.0394 \pm 0.0096, \\ a_2 &= -0.0355 \pm 0.0556, \end{aligned} \tag{60}$$

and the corresponding correlation matrix ($i, j = 1, 2, 3$) is:

$$r_{ij} = \begin{pmatrix} 1 & 0.72 & -0.82 \\ 0.72 & 1 & -0.96 \\ -0.82 & -0.96 & 1 \end{pmatrix}. \tag{61}$$

One sees again strong correlations among all the fitted parameters, which can be well approximated by linear correlations.

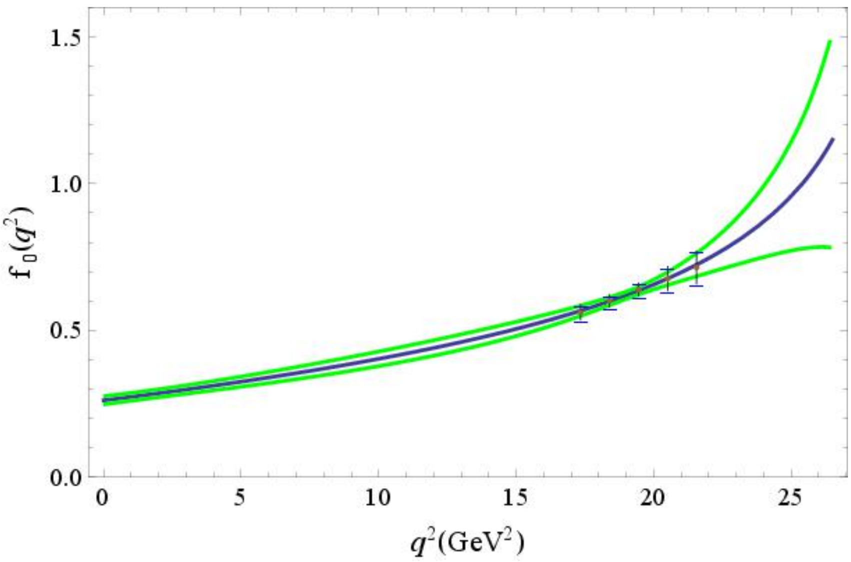

Figure 8: (Color online) The scalar $B \to \pi$ transition form factor $f_0(q^2)$ in the entire kinematic region using the BGL parametrization. The solid green lines show the uncertainty in the form factor. The vertical bars are the Lattice-QCD data [58] used for fixing the form-factor shape.

5.2 The $f_T(q^2)$ Form Factor

As already mentioned, there is at present only scant information about the $B \to \pi$ tensor form factor $f_T^{B\pi}(q^2)$. So, one needs to find a reliable method to extract it from the existing model-independent data. We use an $SU(3)_F$-symmetry-breaking Ansatz involving the both $B \to K$ and $B \to \pi$ form factors. We recall that all three $B \to K$ transition form factors $f_+^{BK}(q^2)$, $f_0^{BK}(q^2)$ and $f_T^{BK}(q^2)$ have been calculated recently by the HPQCD collaboration [20, 21] and the two $B \to \pi$ transition form factors $f_+^{B\pi}(q^2)$ and $f_0^{B\pi}(q^2)$ are also known [58]. Of course, lattice results are available only in the small-recoil limit. With this knowledge, we first estimate the $SU(3)_F$-symmetry-breaking corrections in the already known vector and scalar form factors and use these corrections to estimate the $B \to \pi$ tensor form factor $f_T^{B\pi}(q^2)$ from the corresponding $B \to K$ transition form factor $f_T^{BK}(q^2)$. We introduce the following measures of the $SU(3)_F$-breaking corrections in the transition form factors:

$$R_i(q^2) = \frac{f_i^{BK}(q^2)}{f_i^{B\pi}(q^2)} - 1, \tag{62}$$

where $i = +,\, 0,\, T$. The curves for the $SU(3)_F$-symmetry breaking functions $R_+(q^2)$ and $R_0(q^2)$, calculated for the central values of the form factors from the lattice for small-recoil region, are presented in Fig. 9. As expected, breaking effects of order 10% are seen in both the ratios. We also expect that the $SU(3)_F$-symmetry breaking effect in the third ratio, $R_T(q^2)$, is of the same order. For the sake of definiteness, we assume that the ratio

Table 4: Values of the tensor form factor $f_T^{B\pi}(q^2)$ at the indicated values of q^2 obtained from the existing Lattice-QCD data on the $f_T^{BK}(q^2)$ transition form factor [21] and the $SU(3)_F$-symmetry breaking function $R_T(q^2)$ defined in the text. The variance of $f_T^{B\pi}(q^2)$ is calculated by adding the errors of $f_T^{BK}(q^2)$ and $R_T(q^2)$ in quadrature.

q^2, GeV^2	18.4	19.1	19.8	20.6
$f_T^{BK}(q^2)$	1.197 ± 0.047	1.307 ± 0.051	1.434 ± 0.057	1.608 ± 0.069
$R_T(q^2)$	0.080 ± 0.021	0.076 ± 0.021	0.073 ± 0.023	0.071 ± 0.023
$f_T^{B\pi}(q^2)$	1.108 ± 0.126	1.215 ± 0.115	1.337 ± 0.117	1.503 ± 0.123
q^2, GeV^2	21.3	22.1	22.8	23.5
$f_T^{BK}(q^2)$	1.793 ± 0.082	2.054 ± 0.106	2.342 ± 0.135	2.713 ± 0.176
$R_T(q^2)$	0.070 ± 0.037	0.072 ± 0.050	0.076 ± 0.067	0.083 ± 0.090
$f_T^{B\pi}(q^2)$	1.675 ± 0.144	1.916 ± 0.169	2.178 ± 0.211	2.506 ± 0.302

$R_T(q^2)$ of the tensor form factors is the average of the other two: $R_+(q^2)$ and $R_0(q^2)$,

$$R_T(q^2) = \frac{1}{2}\left[R_+(q^2) + R_0(q^2)\right]. \tag{63}$$

The corresponding function $R_T(q^2)$ is presented in Fig. 9 as the central curve. Explicit values of of this function in the small-recoil region are presented in Table 4. The errors reflect the uncertainties of the lattice calculations and we assume that the errors in the $B \to \pi$ and $B \to K$ transition form factors are uncorrelated.

The values of the $f_T^{B\pi}(q^2)$ form factor were then obtained by rescaling them from the known values of the $f_T^{BK}(q^2)$ form factor [21] by utilizing the relation:

$$f_T^{B\pi}(q^2) = \frac{f_T^{BK}(q^2)}{1 + R_T(q^2)} \,. \tag{64}$$

They are presented in Table 4. The variance of $f_T^{B\pi}(q^2)$ is calculated by adding the errors of $f_T^{BK}(q^2)$ and $R_T(q^2)$ in quadrature. The normalization at $q^2 = 0$: $f_T^{B\pi}(0) = 0.231 \pm 0.013$, which results from $f_+^{B\pi}(0) = 0.261 \pm 0.014$, extracted by us from the experimental data on $B \to \pi \ell \nu_\ell$, and the Heavy-Quark Symmetry relation between the form factors in the large-recoil limit of the π-meson [27, 34]: $f_T^{B\pi}(0) = (1 + m_\pi/m_B)\, f_+^{B\pi}(0)$. With all this at hand, we have a fairly constrained model for the $f_T^{B\pi}(q^2)$ form factor.

For the BGL parametrization of the $f_T^{B\pi}(q^2)$ form factor, the set of fitted parameters entering the expansion in $z(q^2, q_0^2)$ and truncated at $k_{\max} = 2$ is as follows:

$$\begin{aligned} a_0 &= 0.0458 \pm 0.0027, \\ a_1 &= -0.0234 \pm 0.0124, \\ a_2 &= -0.2103 \pm 0.1052, \end{aligned} \tag{65}$$

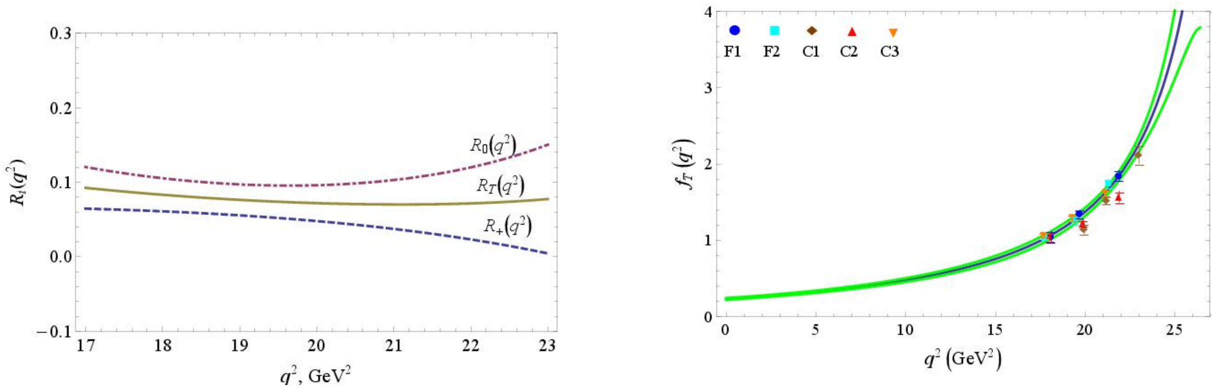

Figure 9: (Color online) The $SU(3)_F$-symmetry breaking functions $R_+(q^2)$, $R_0(q^2)$ and $R_T(q^2)$ (left plot) in the q^2-range accessible by the Lattice-QCD simulations and the tensor $B \to \pi$ transition form factor $f_T(q^2)$ (right plot) in the entire kinematic region. The sets of vertical bars in the large-q^2 region are the preliminary results from the HPQCD Collaboration [24] presented at the Lattice-2013 Conference. The legend on the right plot specifies the lattice ensembles as used in the $B \to K$ transitions [21], by the HPQCD collaboration.

with the corresponding correlation matrix ($i, j = 1, 2, 3$):

$$r_{ij} = \begin{pmatrix} 1 & 0.68 & -0.90 \\ 0.68 & 1 & -0.83 \\ -0.90 & -0.83 & 1 \end{pmatrix}. \tag{66}$$

Strong correlations among the fitted parameters are observed similar to the case of $f_0^{B\pi}(q^2)$.

The resulting $f_T^{B\pi}(q^2)$ form factor is shown in Fig. 9. Recent preliminary results for this form factor at large q^2 from the HPQCD Collaboration [24] are also presented in this figure.[7] The symbols (F1, F2, C1, C2, C3) and the corresponding lattice-data points denote the various lattice ensembles used by this collaboration for performing the numerical simulations, which are the same as the ones used in the calculation of the $B \to K$ transition form factors [20, 21], namely the MILC 2 + 1 asqtad gauge configurations. Good agreement of the lattice data on $f_T^{B\pi}(q^2)$ in the large-q^2 region with our results based on using the $SU(3)_F$-symmetry-breaking Ansatz is evident in this figure.

As all the form factors in the $B \to \pi$ transition are now determined, using data and lattice QCD, we can now make model-independent predictions for the dilepton invariant-mass spectrum and the decay width in the semileptonic $B \to \pi\, \ell^+\ell^-$ decays.

[7]They were presented by C. Bouchard *et al.* at the Lattice-2013 Conference, held recently in Mainz (Germany).

6 $B^+ \to \pi^+\ell^+\ell^-$ Decay in the Low-q^2 Region

6.1 HQS Limit

As discussed in the introduction, one can apply the heavy-quark symmetry (HQS) techniques to relate the form factor $f_T^{B\pi}(q^2)$ in $B^\pm \to \pi^\pm\ell^+\ell^-$ to the one measured form factor $f_+(q^2)$ in the charged-current decay $B \to \pi\ell\nu_\ell$, in the large-recoil (or low-q^2) region. As shown in Ref. [34], in the HQS limit (i. e., without taking into account symmetry-breaking corrections), $f_0(q^2)$ and $f_T(q^2)$ are proportional to $f_+(q^2)$:

$$f_0(q^2) = \frac{m_B^2 - q^2}{m_B^2}\, f_+(q^2), \tag{67}$$

$$f_T(q^2) = \frac{m_B + m_\pi}{m_B}\, f_+(q^2). \tag{68}$$

In the symmetry limit, there is only one independent form factor $f_+(q^2)$, the shape of which can be extracted from the analysis of the $B^0 \to \pi^+\ell^+\nu_\ell$ and $B^+ \to \pi^0\ell^+\nu_\ell$, which we presented earlier. The decay rate of $B^+ \to \pi^+\ell^+\ell^-$ in the HQS limit is greatly simplified and takes the form:

$$\frac{d\mathcal{B}\,(B^+ \to \pi^+\ell^+\ell^-)}{dq^2} = \frac{G_F^2\alpha_{\rm em}^2\tau_{B^+}}{1024\pi^5 m_B^3}\, |V_{tb}V_{td}^*|^2\, \sqrt{\lambda(q^2)}\sqrt{1 - \frac{4m_\ell^2}{q^2}}\, \tilde{F}(q^2)\, f_+^2(q^2), \tag{69}$$

where the dynamical function $F(q^2)$, defined in Eq. (19), is now reduced to the following expression:

$$\begin{aligned}\tilde{F}(q^2) &= \frac{2}{3}\,\lambda(q^2)\left(1 + \frac{2m_\ell^2}{q^2}\right)\left|C_9^{\rm eff}(q^2) + \frac{2m_b}{m_B}\, C_7^{\rm eff}(q^2)\right|^2 + \frac{2}{3}\,\lambda(q^2)\,\left|C_{10}^{\rm eff}\right|^2 \\ &+ \frac{4m_\ell^2}{q^2}\,\left|C_{10}^{\rm eff}\right|^2\left[\left(1 - \frac{m_\pi^2}{m_B^2}\right)^2\left(m_B^2 - q^2\right)^2 - \frac{2}{3}\,\lambda(q^2)\right],\end{aligned} \tag{70}$$

and the kinematic function $\lambda(q^2)$ is given in (18).

Restricting ourselves to the NLL results for the effective Wilson coefficients (i. e., dropping the $\alpha_s(\mu)$-dependent terms in them) and using the $f_+(q^2)$ form-factor shape extracted in terms of the BGL parametrization from the combined BaBar and Belle data, and the numerical values of the different quantities entering (69) from Table 5, the numerical values of the $B^\pm \to \pi^\pm\mu^+\mu^-$ partial branching ratio in the ranges $4m_\mu^2 \leq q^2 \leq$ 8 GeV^2 and 1 GeV$^2 \leq q^2 \leq 8$ GeV^2 are given below:

$$\mathcal{B}(B^\pm \to \pi^\pm\mu^+\mu^-;\, 0.05\,{\rm GeV}^2 \leq q^2 \leq 8\,{\rm GeV}^2) = (0.80 \pm 0.07) \times 10^{-8}, \tag{71}$$

$$\mathcal{B}(B^\pm \to \pi^\pm\mu^+\mu^-;\, 1\,{\rm GeV}^2 \leq q^2 \leq 8\,{\rm GeV}^2) = (0.72 \pm 0.06) \times 10^{-8}. \tag{72}$$

Table 5: Main input parameters used in the theoretical evaluations of the $B^+ \to \pi^+\ell^+\ell^-$ branching fractions taken from the PDG [26], except for the B-meson leptonic decay constant f_B, whose value is taken from lattice-NRQCD [59].

$G_F = 1.11637 \times 10^{-5}\,\text{GeV}^{-2}$	$\alpha_{\text{em}}^{-1} = 129$
$\alpha_s(M_Z) = 0.1184 \pm 0.0007$	$f_B = (184 \pm 4)$ GeV
$m_c(m_c) = (1.275 \pm 0.025)$ GeV	$m_b(m_b) = (4.18 \pm 0.03)$ GeV
$\lambda = 0.22535 \pm 0.00065$	$A = 0.817 \pm 0.015$
$\bar{\rho} = 0.136 \pm 0.018$	$\bar{\eta} = 0.348 \pm 0.014$
$\lvert V_{ud}\rvert = 0.97427$	$\lvert V_{tb}\rvert = 0.999146$
$\lvert V_{ub}\rvert = (3.51^{+0.15}_{-0.14}) \times 10^{-3}$	$\lvert V_{td}\rvert = (8.67^{+0.29}_{-0.31}) \times 10^{-3}$

6.2 Including HQS-Breaking Correction

Both heavy-quark symmetry and final hadron kinematics in the large-recoil limit allows to get relations among the $B \to \pi$ form factors [27]. With taking into account symmetry-breaking corrections, these relations were worked out in Ref. [34]:

$$
\begin{aligned}
f_0(q^2) &= \left(1 - \frac{q^2}{m_B^2}\right) f_+(q^2) \left\{1 + \frac{C_F \alpha_s(\mu_h)}{4\pi} \left[2 - 2L(q^2)\right]\right\} \\
&+ \frac{C_F \alpha_s(\mu_{hc})}{4\pi} \frac{q^2}{m_B^2 - q^2} \Delta F_\pi,
\end{aligned}
\tag{73}
$$

$$
\begin{aligned}
f_T(q^2) &= \left(1 + \frac{m_\pi}{m_B}\right) f_+(q^2) \left[1 + \frac{C_F \alpha_s(\mu_h)}{4\pi} \left(\ln \frac{m_b^2}{\mu_h^2} + 2L(q^2)\right)\right] \\
&- \frac{C_F \alpha_s(\mu_{hc})}{4\pi} \frac{m_B\,(m_B + m_\pi)}{m_B^2 - q^2} \Delta F_\pi,
\end{aligned}
\tag{74}
$$

where $C_F = 4/3$. The strong coupling $\alpha_s(\mu)$ depends on the specific scales of the contributing diagrams, which we take as the hard $\mu_h \sim m_b$ and hard-collinear $\mu_{hc} \sim \sqrt{m_b \Lambda}$ scales, where $\Lambda \simeq 0.5$ GeV is the typical soft hadronic scale. The auxiliary function $L(q^2)$ is defined as [34]:

$$
L(q^2) = \left(1 - \frac{m_B^2}{q^2}\right) \ln \left(1 - \frac{q^2}{m_B^2}\right),
\tag{75}
$$

with the normalization $L(0) = 1$, and the contributions of the hard-spectator diagrams are parametrized by the quantity [34]:

$$
\Delta F_\pi = \frac{8\pi^2 f_B f_\pi}{3 m_B} \left\langle l_+^{-1} \right\rangle_+ \left\langle \bar{u}^{-1} \right\rangle_\pi .
\tag{76}
$$

Here, f_B and f_π are the leptonic decay constants of the B- and π-mesons and the following first inverse moments of the B- and π-mesons are used:

$$\left\langle l_+^{-1} \right\rangle_+ = \int\limits_0^\infty dl_+ \, \frac{\phi_+^B(l_+)}{l_+}, \quad \left\langle \bar{u}^{-1} \right\rangle_\pi = \int\limits_0^1 du \, \frac{\phi_\pi(u)}{1-u}, \tag{77}$$

which are completely determined by the leading-twist light-cone distribution amplitudes $\phi_+^B(l_+)$ [60,61] and $\phi_\pi(u)$ [62–70]. With the input parameters m_B, f_B and f_π from Table 5, the values of moments $\langle \bar{u}^{-1} \rangle_\pi (1 \text{ GeV}) = 3.30 \pm 0.42$ and $\left\langle l_+^{-1} \right\rangle_+ (1.5 \text{ GeV}) = (1.86 \pm 0.17) \text{ GeV}^{-1}$ [71], the value of (76) is estimated as $\Delta F_\pi = 0.74 \pm 0.12$. We note that this is smaller than $\Delta F_\pi = 1.17$ used in Ref. [34]. This difference reflects the observation that the π-meson is well described by the asymptotic form of the twist-2 LCDA $\phi_\pi(u) = 6u\,(1-u)$, and the first subleading Gegenbauer moment $a_2(1 \text{ GeV}) = 0.10 \pm 0.14$ [72] is consistent with zero.

Taking into account the symmetry-breaking corrections, and the NNLO effects in the effective Wilson coefficients, the partial branching fractions, integrated in the ranges of q^2 as in (71) and (72), are decreased. We get

$$\mathcal{B}(B^+ \to \pi^+ \mu^+ \mu^-;\, 0.05\,\text{GeV}^2 \le q^2 \le 8\,\text{GeV}^2) = (0.65^{+0.08}_{-0.06}) \times 10^{-8}, \tag{78}$$
$$\mathcal{B}(B^+ \to \pi^+ \mu^+ \mu^-;\, 1\,\text{GeV}^2 \le q^2 \le 8\,\text{GeV}^2) = (0.57^{+0.07}_{-0.05}) \times 10^{-8}, \tag{79}$$

which mainly reflects the NNLO effects in the Wilson coefficients. The corresponding dilepton invariant-mass distribution in the large-recoil approximation ($q^2 \le 8$ GeV^2) is shown in Fig. 10. The vertical line shows the light-resonance (ρ, ω, and ϕ) region collectively. The upper bound on q^2 is imposed to avoid the large (resonant) contribution from the long-distance process $B^\pm \to \pi^\pm J/\psi \to \pi^\pm \ell^+ \ell^-$.

7 $B^+ \to \pi^+ \ell^+ \ell^-$ Decay in the Entire q^2-Range

In the low hadronic-recoil region (large-q^2), heavy-quark symmetry does not hold, and we have three independent form factors $f_+(q^2)$, $f_0(q^2)$ and $f_T(q^2)$ in $B^\pm \to \pi^\pm \ell^+ \ell^-$. We have given a detailed account of their determination in the preceding sections, taking into account the Belle and BaBar data on $B \to \pi \ell \nu_\ell$, heavy-quark symmetry and its leading-order breaking (for $q^2 \le 8$ GeV^2) and Lattice-QCD results in the large-q^2 region, obtained for the $B \to K$ and $B \to \pi$ transitions.

Before presenting our numerical results, we discuss the choice for the parameter $\sqrt{z} = m_c/m_b$ entering the NNLO corrections. The NNLO corrections to the $b \to s\,\ell^+\ell^-$ transition matrix element [42], which we have adapted for the exclusive $b \to d\,\ell^+\ell^-$ case discussed by us here, are available in the literature both as a Mathematica and a C++ programs [42], from which the former one was implemented into our own Mathematica routine. We need to fix this ratio in terms of the c- and b-quark pole masses. The three-loop relation between the pole m_{pole} and $\overline{\text{MS}}$-scheme $\bar{m}(\bar{m})$ masses [73–75] can be used to get the c- and b-quark pole masses. Staring from the values collected in Table 5, the ratio

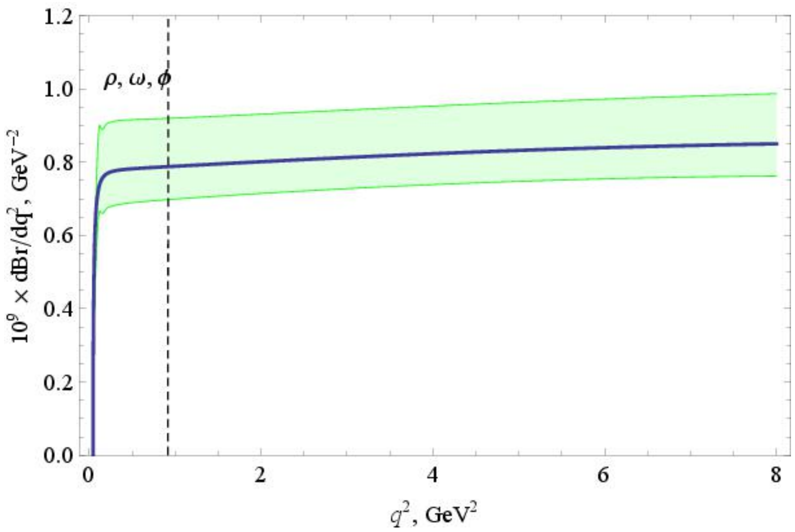

Figure 10: The dilepton invariant-mass distribution $d\mathcal{B}(B^\pm \to \pi^\pm \ell^+\ell^-)/dq^2$ for $0 \le q^2 \le 8$ GeV^2 calculated by taking into account the leading HQS-breaking corrections. Dashed vertical line indicates collectively the vector ρ-, ω-, and ϕ-resonance region.

$m_c(m_c)/m_b(m_b) = 0.305 \pm 0.006$ can be transformed into the ratio of the pole masses $m_{c,\text{pole}}/m_{b,\text{pole}} = 0.402 \pm 0.008$. In another work [76], additional electroweak corrections to the relation between the pole and $\overline{\text{MS}}$ quark masses were taken into account with the resulting pole masses: $m_{c,\text{pole}} = 1.77 \pm 0.14$ GeV and $m_{b,\text{pole}} = 4.91 \pm 0.12$ GeV, with the ratio $m_{c,\text{pole}}/m_{b,\text{pole}} = 0.36 \pm 0.03$. This value is used by us as the input for $\sqrt{z}$ in calculating the c-quark loop-induced corrections.

The invariant-mass spectrum in the entire range of q^2 ($4m_\ell^2 < q^2 < 26.4$ GeV^2) is presented in Fig. 11. The dashed vertical lines specify the resonant regions of light mesons at $q^2 \lesssim 1$ GeV^2 as well as of J/ψ- and $\psi(2S)$-mesons. As mentioned earlier, in the calculation of this spectrum the Wilson coefficients in NNLO and the model-independent $f_+(q^2)$ and $f_T(q^2)$ form factors were used. As the auxiliary functions $F_{1,2}^{(7)}(q^2)$ and $F_{1,2}^{(9)}(q^2)$ entering the next-to-leading correction in $C_9^{\text{eff}}(q^2)$ are known analytically as the power expansions in $s = q^2/m_B^2$ and in $1 - s$ (as shown in Fig. 2) we have extrapolated these functions into the intermediate q^2-region. In doing this, we have matched the known analytical functions in the form of expansions at the "matching" point $q^2 \simeq 12.5$ GeV^2, at which value the spectrum has the minimal discontinuity (see Fig. 11). This results into an invariant-mass spectrum which is a smooth function in q^2, within uncertainties. It is important to note that the "matching" point $q^2 \simeq 12.5$ GeV^2 lies in the $\psi(2S)$-resonance region which is dominated by the long-distance effects and the short-distance analysis performed by us is not valid. After excluding the resonance regions, the short-distance contribution to the differential branching fraction dominates and the discontinuity in the spectrum is not crucial. This allows us to make a prediction for the partial branching fraction also in the gap between the J/ψ- and $\psi(2S)$-resonances (a similar quantity has been measured in the $B \to K\,\ell^+\ell^-$ decays) but this estimate should be taken with caution as possible long-distance effects, being sub-dominant, nevertheless could change the value

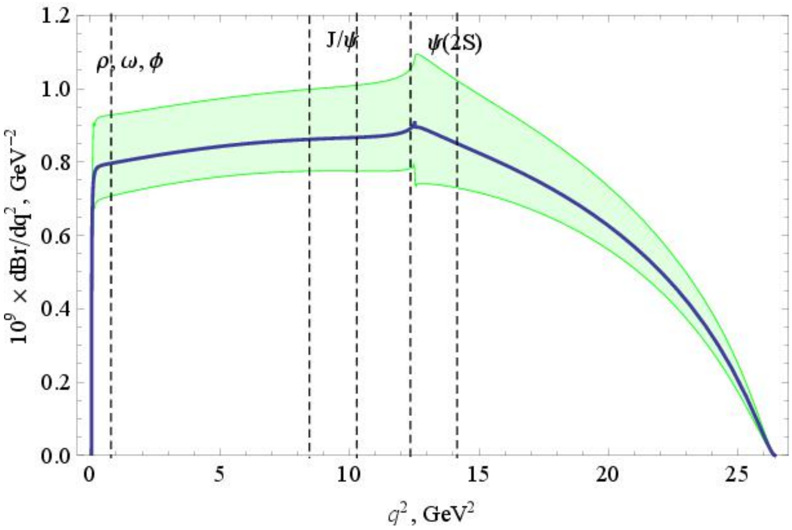

Figure 11: The dilepton invariant-mass distribution in the $B^+ \to \pi^+\ell^+\ell^-$ decay for the entire kinematic range $0 \leq q^2 \leq 26.4$ GeV^2. Dashed vertical lines specify the positions of vector resonances: ρ-, ω- and ϕ-mesons at $q^2 \lesssim 1$ GeV^2 and J/ψ- and $\psi(2S)$-mesons near $q^2 \simeq 9.5$ GeV^2 and $q^2 \simeq 13.5$ GeV^2, respectively.

substantially.

Our predictions for the partial branching fractions $d\mathcal{B}(B^\pm \to \pi^\pm \ell^+\ell^-)/dq^2$ in eleven different q^2 bins are presented in Table 6. The total branching fraction of the semileptonic $B^\pm \to \pi^\pm \mu^+\mu^-$ decay is as follows:

$$\begin{aligned} \mathcal{B}(B^\pm \to \pi^\pm \mu^+\mu^-) &= \Big(1.88^{+0.28}_{-0.15}\big|_{\mu_b} \pm 0.13\big|_{|V_{td}|} \pm 0.08\big|_{\rm FF} \pm 0.01\Big) \times 10^{-8} \\ &= \big(1.88^{+0.32}_{-0.21}\big) \times 10^{-8}, \end{aligned} \tag{80}$$

where the individual uncertainties are from the scale dependence μ_b of the Wilson coefficients, the CKM matrix element $|V_{td}|$ and form factors (FF), as indicated. The resulting average uncertainty about 15% is dominated by the scale dependence of the Wilson coefficients and can be reduced after the scale-dependence of the tensor form factor $f_T^{B\pi}(q^2)$ is worked out properly in the entire q^2-range.

The branching fraction for the semileptonic $B^\pm \to \pi^\pm e^+e^-$ decay is the same as (80), as the additional contribution induced by the shift to the lower kinematic values of $q^2 = m_e^2 \simeq 0.26$ MeV^2 is negligible.

8 Summary and Outlook

We have presented a theoretically improved calculation of the branching fraction for the $B^\pm \to \pi^\pm\mu^+\mu^-$ decay, measured recently by the LHCb collaboration [1]. In doing this, we have used the effective Wilson coefficients $C_7^{\rm eff}(q^2)$, $C_9^{\rm eff}(q^2)$ and $C_{10}^{\rm eff}$, obtained in the NNLO accuracy earlier for the $b \to (s,\, d)\,\ell^+\ell^-$ decays [33, 35–38]. Some of the auxiliary

Table 6: Partial branching ratios $d\mathcal{B}(B^+ \to \pi^+\mu^+\mu^-)/dq^2$ integrated over the indicated ranges $[q^2_{\rm min}, q^2_{\rm max}]$.

$[q^2_{\rm min}, q^2_{\rm max}]$	$10^8 \times \mathcal{B}(q^2_{\rm min} \leq q^2 \leq q^2_{\rm max})$
$[0.05, 2.0]$	$0.15^{+0.03}_{-0.02}$
$[1, 2.0]$	$0.08^{+0.01}_{-0.01}$
$[2.0, 4.3]$	$0.19^{+0.03}_{-0.02}$
$[4.3, 8.68]$	$0.37^{+0.06}_{-0.04}$
$[10.09, 12.86]$	$0.25^{+0.04}_{-0.03}$
$[14.18, 16.0]$	$0.15^{+0.03}_{-0.02}$
$[16.0, 18.0]$	$0.15^{+0.03}_{-0.02}$
$[18.0, 22.0]$	$0.25^{+0.04}_{-0.03}$
$[22.0, 26.4]$	$0.13^{+0.02}_{-0.02}$
$[0.05, 8.0]$	$0.66^{+0.10}_{-0.07}$
$[1.0, 8.0]$	$0.58^{+0.09}_{-0.06}$
$[4m_\mu^2, (m_B - m_\pi)^2]$ (total)	$1.88^{+0.32}_{-0.21}$

functions, called $F^{(7)}_{1,2}(q^2)$, $F^{(9)}_{1,2}(q^2)$, $F^{(7)}_{1,(2),u}(q^2)$, $F^{(9)}_{1,(2),u}(q^2)$ are known analytically in the limiting case of $m_c/m_b = 0$ [41], which we have used. For realistic values of this ratio, taken by us as $\sqrt{z} = m_c/m_b = 0.36$, the results are known only in limited ranges of $s = q^2/m_B^2$ ($s \leq 0.35$ and $0.55 < s < 1.0$). All these functions are shown numerically in Fig. 2. We have interpolated in the gap, which introduces some uncertainty, but being part of the NNLO contribution, it is not expected to be the dominant error. Theoretical uncertainties are dominated by the imprecise knowledge of the form factors, $f_+^{B\pi}(q^2)$ and $f_T^{B\pi}(q^2)$. We have extracted the shape the former from data on the charged-current process $B \to \pi\ell\nu_\ell$, measured at the B-factories. Among the four popular parametrizations, the BGL one (z-expansion) was chosen as the working tool. For the tensor form factor $f_T^{B\pi}(q^2)$, heavy-quark symmetry provides the information in the low-q^2 (large-recoil) region, in which this form factor is related to the known factor $f_+^{B\pi}(q^2)$, up to symmetry-breaking effects, which we have estimated from the existing literature. This provides us an estimate of the dilepton invariant-mass spectrum for $q^2 \leq 8$ GeV^2. For larger values of q^2, we have used the $SU(3)_F$-symmetry-breaking Ansatz and knowledge of the form factor $f_T^{BK}(q^2)$. Comparison with the preliminary results by the HPQCD collaboration studies of the form factor $f_T^{B\pi}(q^2)$ in the low-recoil (or large-q^2) region [24] shows a good consistency of our findings. This then provides us a trustworthy profile of the two form factors needed in estimating the entire dilepton invariant-mass spectrum and the partial branching ratio. The combined accuracy on the branching ratio is estimated as $\pm 15\%$, and the resulting branching fraction $\mathcal{B}(B^\pm \to \pi^\pm\mu^+\mu^-) = (1.88^{+0.32}_{-0.21}) \times 10^{-8}$ is in agreement with the LHCb data [1]. We have provided partial branching fractions in different ranges of q^2, which can be compared directly with the data, as and when they become available.

Acknowledgments

A. R. would like to thank Wei Wang and Christian Hambrock for helpful discussions on technical details of the calculations performed and the Theory Group at DESY for the kind and generous hospitality. We acknowledge helpful communications with Ran Zhou of the FermiLab and MILC collaborations on the lattice results. The work of A. R. is partially supported by the German-Russian Interdisciplinary Science Center (G-RISC) funded by the German Federal Foreign Office via the German Academic Exchange Service (DAAD) under the project No. P-2013a-9.

References

[1] R. Aaij, et al., First observation of the decay $B^+ \to \pi^+\mu^+\mu^-$, JHEP 1212 (2012) 125. arXiv:1210.2645, doi:10.1007/JHEP12(2012)125.

[2] Y. Amhis, et al., Averages of b-hadron, c-hadron, and τ-lepton properties as of early 2012, arXiv:1207.1158.

[3] J.-J. Wang, R.-M. Wang, Y.-G. Xu, Y.-D. Yang, The Rare decays $B_u^+ \to \pi^+\ell^+\ell^-$, $\rho^+\ell^+\ell^-$ and $B_d^0 \to \ell^+\ell^-$, in the R-parity violating supersymmetry, Phys. Rev. D77 (2008) 014017. arXiv:0711.0321, doi:10.1103/PhysRevD.77.014017.

[4] H.-Z. Song, L.-X. Lu, G.-R. Lu, New physics effects on rare decays $B_u^+ \to \pi^+\ell^+\ell^-$, $\rho^+\ell^+\ell^-$ in a top quark two-Higgs-doublet model, Commun. Theor. Phys. 50 (2008) 696–702. doi:10.1088/0253-6102/50/3/35.

[5] W.-F. Wang, Z.-J. Xiao, The semileptonic decays $B/B_s \to (\pi, K)(\ell^+\ell^-, \ell\nu, \nu\bar{\nu})$ in the perturbative QCD approach beyond the leading-order, Phys. Rev. D86 (2012) 114025. arXiv:1207.0265, doi:10.1103/PhysRevD.86.114025.

[6] P. Ball, R. Zwicky, New results on $B \to \pi, K, \eta$ decay formfactors from light-cone sum rules, Phys. Rev. D71 (2005) 014015. arXiv:hep-ph/0406232, doi:10.1103/PhysRevD.71.014015.

[7] G. Duplancic, A. Khodjamirian, T. Mannel, B. Melic, N. Offen, Light-cone sum rules for $B \to \pi$ form factors revisited, JHEP 0804 (2008) 014. arXiv:0801.1796, doi:10.1088/1126-6708/2008/04/014.

[8] P. del Amo Sanchez, et al., Study of $B \to \pi\ell\nu$ and $B \to \rho\ell\nu$ Decays and Determination of $|V_{ub}|$, Phys. Rev. D83 (2011) 032007. arXiv:1005.3288, doi:10.1103/PhysRevD.83.032007.

[9] J. Lees, et al., Branching fraction measurement of $B \to \omega\ell\nu$ decays, Phys. Rev. D87 (2013) 032004. arXiv:1205.6245, doi:10.1103/PhysRevD.87.032004.

[10] H. Ha, et al., Measurement of the decay $B^0 \to \pi^- \ell^+ \nu$ and determination of $|V_{ub}|$, Phys. Rev. D83 (2011) 071101. arXiv:1012.0090, doi:10.1103/PhysRevD.83.071101.

[11] A. Sibidanov, et al., Study of Exclusive $B \to X_u \ell \nu$ Decays and Extraction of $|V_{ub}|$ using Full Reconstruction Tagging at the Belle Experiment, Phys. Rev. D88 (2013) 032005. arXiv:1306.2781, doi:10.1103/PhysRevD.88.032005.

[12] D. Becirevic, A. B. Kaidalov, Comment on the heavy $\to$ light form-factors, Phys. Lett. B478 (2000) 417–423. arXiv:hep-ph/9904490, doi:10.1016/S0370-2693(00)00290-2.

[13] C. G. Boyd, B. Grinstein, R. F. Lebed, Constraints on form-factors for exclusive semileptonic heavy-to-light meson decays, Phys. Rev. Lett. 74 (1995) 4603–4606. arXiv:hep-ph/9412324, doi:10.1103/PhysRevLett.74.4603.

[14] C. Bourrely, I. Caprini, L. Lellouch, Model-independent description of $B \to \pi \ell \nu$ decays and a determination of $|V_{ub}|$, Phys. Rev. D79 (2009) 013008. arXiv:0807.2722, doi:10.1103/PhysRevD.82.099902,10.1103/PhysRevD.79.013008.

[15] T. Becher, R. J. Hill, Comment on form-factor shape and extraction of $|V_{ub}|$ from $B \to \pi \ell \nu$, Phys. Lett. B633 (2006) 61–69. arXiv:hep-ph/0509090, doi:10.1016/j.physletb.2005.11.063.

[16] R. Zhou, Lattice Calculations of $B \to K/K^* \ell^+ \ell^-$ form factors, arXiv:1301.0666.

[17] A. Bazavov, D. Toussaint, C. Bernard, J. Laiho, C. DeTar, et al., Nonperturbative QCD simulations with 2 + 1-flavors of improved staggered quarks, Rev. Mod. Phys. 82 (2010) 1349–1417. arXiv:0903.3598, doi:10.1103/RevModPhys.82.1349.

[18] R. Zhou, et al., Form Factors for $B \to K \ell \ell$ Semileptonic Decay from Three-Flavor Lattice QCD, PoS LATTICE-2011 (2011) 298. arXiv:1111.0981.

[19] R. Zhou, S. Gottlieb, J. A. Bailey, D. Du, A. X. El-Khadra, et al., Form factors for semi-leptonic B-decays, PoS LATTICE-2012 (2012) 120. arXiv:1211.1390.

[20] C. Bouchard, G. P. Lepage, C. Monahan, H. Na, J. Shigemitsu, Standard Model predictions for $B \to K \ell \ell$ with form factors from lattice QCD, Phys. Rev. Lett. 111 (2013) 162002. arXiv:1306.0434, doi:10.1103/PhysRevLett.111.162002.

[21] C. Bouchard, G. P. Lepage, C. Monahan, H. Na, J. Shigemitsu, The rare decay $B \to K \ell \ell$ form factors from lattice QCD, Phys. Rev. D88 (2013) 054509. arXiv:1306.2384, doi:10.1103/PhysRevD.88.054509.

[22] Z. Liu, S. Meinel, A. Hart, R. R. Horgan, E. H. Muller, et al., Form factors for rare B-decays: Strategy, methodology, and numerical study, PoS LAT2009 (2009) 242. arXiv:0911.2370.

[23] Z. Liu, S. Meinel, A. Hart, R. R. Horgan, E. H. Muller, et al., A Lattice calculation of $B \to K^{(*)}$ form factors, arXiv:1101.2726.

[24] C. Bouchard, G. P. Lepage, C. J. Monahan, H. Na, J. Shigemitsu, B and B_s semileptonic decay form factors with NRQCD/HISQ quarks, arXiv:1310.3207.

[25] D. Du, J. A. Bailey, A. Bazavov, C. Bernard, A. El-Khadra, et al., $B \to \pi\ell\nu$ and $B \to \pi\ell^+\ell^-$ semileptonic form factors from unquenched lattice QCD, PoS LATTICE-2013 (2013) 383. arXiv:1311.6552.

[26] J. Beringer, et al., Review of Particle Physics (RPP), Phys. Rev. D86 (2012) 010001. doi:10.1103/PhysRevD.86.010001.

[27] J. Charles, A. Le Yaouanc, L. Oliver, O. Pene, J. Raynal, Heavy-to-light form factors in the final hadron large energy limit of QCD, Phys. Rev. D60 (1999) 014001. arXiv:hep-ph/9812358, doi:10.1103/PhysRevD.60.014001.

[28] M. Beneke, T. Feldmann, D. Seidel, Systematic approach to exclusive $B \to V\ell^+\ell^-$, $V\gamma$ decays, Nucl. Phys. B612 (2001) 25–58. arXiv:hep-ph/0106067, doi:10.1016/S0550-3213(01)00366-2.

[29] C. Bobeth, G. Hiller, D. van Dyk, General Analysis of $\bar{B} \to \bar{K}^{(*)}\ell^+\ell^-$ Decays at Low Recoil, Phys. Rev. D87 (2013) 034016. arXiv:1212.2321, doi:10.1103/PhysRevD.87.034016.

[30] C. Hambrock, G. Hiller, Extracting $B \to K^*$ Form Factors from Data, Phys. Rev. Lett. 109 (2012) 091802. arXiv:1204.4444, doi:10.1103/PhysRevLett.109.091802.

[31] G. Buchalla, A. J. Buras, M. E. Lautenbacher, Weak decays beyond leading logarithms, Rev. Mod. Phys. 68 (1996) 1125–1144. arXiv:hep-ph/9512380, doi:10.1103/RevModPhys.68.1125.

[32] K. G. Chetyrkin, M. Misiak, M. Munz, Weak radiative B-meson decay beyond leading logarithms, Phys. Lett. B400 (1997) 206–219. arXiv:hep-ph/9612313, doi:10.1016/S0370-2693(97)00324-9.

[33] C. Bobeth, M. Misiak, J. Urban, Photonic penguins at two loops and m_t-dependence of BR$[B \to X_s\ell^+\ell^-]$, Nucl. Phys. B574 (2000) 291–330. arXiv:hep-ph/9910220, doi:10.1016/S0550-3213(00)00007-9.

[34] M. Beneke, T. Feldmann, Symmetry-breaking corrections to heavy-to-light B-meson form factors at large recoil, Nucl. Phys. B592 (2001) 3–34. arXiv:hep-ph/0008255, doi:10.1016/S0550-3213(00)00585-X.

[35] H. Asatrian, H. Asatrian, C. Greub, M. Walker, Two-loop virtual corrections to $B \to X_s\ell^+\ell^-$ in the standard model, Phys. Lett. B507 (2001) 162–172. arXiv:hep-ph/0103087, doi:10.1016/S0370-2693(01)00441-5.

[36] H. Asatryan, H. Asatrian, C. Greub, M. Walker, Calculation of two-loop virtual corrections to $b \to s\ell^+\ell^-$ in the standard model, Phys. Rev. D65 (2002) 074004. arXiv:hep-ph/0109140, doi:10.1103/PhysRevD.65.074004.

[37] A. Ali, E. Lunghi, C. Greub, G. Hiller, Improved model independent analysis of semileptonic and radiative rare B decays, Phys. Rev. D66 (2002) 034002. arXiv:hep-ph/0112300, doi:10.1103/PhysRevD.66.034002.

[38] H. Asatrian, K. Bieri, C. Greub, M. Walker, Virtual corrections and bremsstrahlung corrections to $b \to d\ell^+\ell^-$ in the standard model, Phys. Rev. D69 (2004) 074007. arXiv:hep-ph/0312063, doi:10.1103/PhysRevD.69.074007.

[39] L. Wolfenstein, Parametrization of the Kobayashi-Maskawa Matrix, Phys. Rev. Lett. 51 (1983) 1945. doi:10.1103/PhysRevLett.51.1945.

[40] A. Ali, P. Ball, L. Handoko, G. Hiller, Comparative study of the decays $B \to (K, K^*)\ell^+\ell^-$ in standard model and supersymmetric theories, Phys. Rev. D61 (2000) 074024. arXiv:hep-ph/9910221, doi:10.1103/PhysRevD.61.074024.

[41] D. Seidel, Analytic two loop virtual corrections to $b \to d\ell^+\ell^-$, Phys. Rev. D70 (2004) 094038. arXiv:hep-ph/0403185, doi:10.1103/PhysRevD.70.094038.

[42] C. Greub, V. Pilipp, C. Schupbach, Analytic calculation of two-loop QCD corrections to $b \to s\ell^+\ell^-$ in the high q^2-region, JHEP 0812 (2008) 040. arXiv:0810.4077, doi:10.1088/1126-6708/2008/12/040.

[43] A. Ghinculov, T. Hurth, G. Isidori, Y. Yao, The Rare Decay $B \to X_s\ell^+\ell^-$ to NNLL Precision for Arbitrary Dilepton Invariant Mass, Nucl. Phys. B685 (2004) 351–392. arXiv:hep-ph/0312128, doi:10.1016/j.nuclphysb.2004.02.028.

[44] E. B. Gregory, C. T. Davies, I. D. Kendall, J. Koponen, K. Wong, et al., Precise B, B_s, and B_c meson spectroscopy from full lattice QCD, Phys. Rev. D83 (2011) 014506. arXiv:1010.3848, doi:10.1103/PhysRevD.83.014506.

[45] C. G. Boyd, B. Grinstein, R. F. Lebed, Model independent extraction of $|V_{cb}|$ using dispersion relations, Phys. Lett. B353 (1995) 306–312. arXiv:hep-ph/9504235, doi:10.1016/0370-2693(95)00480-9.

[46] C. G. Boyd, B. Grinstein, R. F. Lebed, Model-Independent Determinations of $\bar{B} \to D\ell\bar{\nu}$, $D^*\ell\bar{\nu}$ Form Factors, Nucl. Phys. B461 (1996) 493–511. arXiv:hep-ph/9508211, doi:10.1016/0550-3213(95)00653-2.

[47] C. G. Boyd, B. Grinstein, R. F. Lebed, Precision corrections to dispersive bounds on form-factors, Phys. Rev. D56 (1997) 6895–6911. arXiv:hep-ph/9705252, doi:10.1103/PhysRevD.56.6895.

[48] C. G. Boyd, M. J. Savage, Analyticity, shapes of semileptonic form-factors, and $\bar{B} \to \pi\ell\bar{\nu}$, Phys. Rev. D56 (1997) 303–311. arXiv:hep-ph/9702300, doi:10.1103/PhysRevD.56.303.

[49] A. Bharucha, T. Feldmann, M. Wick, Theoretical and Phenomenological Constraints on Form Factors for Radiative and Semi-Leptonic B-Meson Decays, JHEP 1009 (2010) 090. arXiv:1004.3249, doi:10.1007/JHEP09(2010)090.

[50] L. Lellouch, Lattice constrained unitarity bounds for $\bar{B}^0 \to \pi^+\ell^-\bar{\nu}_\ell$ decays, Nucl. Phys. B479 (1996) 353–391. arXiv:hep-ph/9509358, doi:10.1016/0550-3213(96)00443-9.

[51] C. G. Boyd, R. F. Lebed, Improved QCD form-factor constraints and $\Lambda_b \to \Lambda_c\ell\bar{\nu}$, Nucl. Phys. B485 (1997) 275–290. arXiv:hep-ph/9512363, doi:10.1016/S0550-3213(96)00614-1.

[52] M. C. Arnesen, B. Grinstein, I. Z. Rothstein, I. W. Stewart, A precision model independent determination of $|V_{ub}|$ from $B \to \pi e\nu$, Phys. Rev. Lett. 95 (2005) 071802. arXiv:hep-ph/0504209, doi:10.1103/PhysRevLett.95.071802.

[53] B. L. Ioffe, QCD at low energies, Prog. Part. Nucl. Phys. 56 (2006) 232–277. arXiv:hep-ph/0502148, doi:10.1016/j.ppnp.2005.05.001.

[54] M. Neubert, Heavy quark symmetry, Phys. Rept. 245 (1994) 259–396. arXiv:hep-ph/9306320, doi:10.1016/0370-1573(94)90091-4.

[55] G. Burdman, Z. Ligeti, M. Neubert, Y. Nir, The Decay $B \to \pi\ell\nu$ in Heavy Quark Effective Theory, Phys. Rev. D49 (1994) 2331–2345. arXiv:hep-ph/9309272, doi:10.1103/PhysRevD.49.2331.

[56] P. del Amo Sanchez, et al., Measurement of the $B^0 \to \pi^\ell\ell^+\nu$ and $B^+ \to \eta^{(\prime)}\ell^+\nu$ Branching Fractions, the $B^0 \to \pi^-\ell^+\nu$ and $B^+ \to \eta\ell^+\nu$ Form-Factor Shapes, and Determination of $|V_{ub}|$, Phys. Rev. D83 (2011) 052011. arXiv:1010.0987, doi:10.1103/PhysRevD.83.052011.

[57] J. Lees, et al., Branching fraction and form-factor shape measurements of exclusive charmless semileptonic B-decays, and determination of $|V_{ub}|$, Phys. Rev. D86 (2012) 092004. arXiv:1208.1253, doi:10.1103/PhysRevD.86.092004.

[58] E. Dalgic, A. Gray, M. Wingate, C. T. Davies, G. P. Lepage, et al., B-meson semileptonic form-factors from unquenched lattice QCD, Phys. Rev. D73 (2006) 074502. arXiv:hep-lat/0601021, doi:10.1103/PhysRevD.75.119906,10.1103/PhysRevD.73.074502.

[59] R. Dowdall, C. Davies, R. Horgan, C. Monahan, J. Shigemitsu, B-meson decay constants from improved lattice NRQCD and physical u, d, s and c sea quarks, Phys. Rev. Lett. 110 (2013) 222003. arXiv:1302.2644, doi:10.1103/PhysRevLett.110.222003.

[60] A. Grozin, M. Neubert, Asymptotics of heavy meson form-factors, Phys. Rev. D55 (1997) 272–290. arXiv:hep-ph/9607366, doi:10.1103/PhysRevD.55.272.

[61] V. Braun, D. Y. Ivanov, G. Korchemsky, The B-meson distribution amplitude in QCD, Phys. Rev. D69 (2004) 034014. arXiv:hep-ph/0309330, doi:10.1103/PhysRevD.69.034014.

[62] V. Chernyak, A. Zhitnitsky, Asymptotic Behavior of Hadron Form-Factors in Quark Model, JETP Lett. 25 (1977) 510.

[63] V. Chernyak, A. Zhitnitsky, V. Serbo, Asymptotic hadronic form-factors in quantum chromodynamics, JETP Lett. 26 (1977) 594–597.

[64] V. Chernyak, A. Zhitnitsky, Asymptotics of Hadronic Form-Factors in the Quantum Chromodynamics, Sov. J. Nucl. Phys. 31 (1980) 544–552.

[65] A. Efremov, A. Radyushkin, Factorization and Asymptotical Behavior of Pion Form-Factor in QCD, Phys. Lett. B94 (1980) 245–250. doi:10.1016/0370-2693(80)90869-2.

[66] A. Efremov, A. Radyushkin, Asymptotical Behavior of Pion Electromagnetic Form-Factor in QCD, Theor. Math. Phys. 42 (1980) 97–110. doi:10.1007/BF01032111.

[67] G. P. Lepage, S. J. Brodsky, Exclusive Processes in Quantum Chromodynamics: Evolution Equations for Hadronic Wave Functions and the Form-Factors of Mesons, Phys. Lett. B87 (1979) 359–365. doi:10.1016/0370-2693(79)90554-9.

[68] G. P. Lepage, S. J. Brodsky, Exclusive Processes in Perturbative Quantum Chromodynamics, Phys. Rev. D22 (1980) 2157–2198. doi:10.1103/PhysRevD.22.2157.

[69] V. M. Braun, I. Filyanov, QCD Sum Rules in Exclusive Kinematics and Pion Wave Function, Z. Phys. C44 (1989) 157–166. doi:10.1007/BF01548594.

[70] P. Ball, Theoretical update of pseudoscalar meson distribution amplitudes of higher twist: The Nonsinglet case, JHEP 9901 (1999) 010. arXiv:hep-ph/9812375.

[71] S. J. Lee, M. Neubert, Model-independent properties of the B-meson distribution amplitude, Phys. Rev. D72 (2005) 094028. arXiv:hep-ph/0509350, doi:10.1103/PhysRevD.72.094028.

[72] S. Agaev, V. Braun, N. Offen, F. Porkert, BELLE Data on the $\pi^0\gamma^*\gamma$ Form Factor: A Game Changer?, Phys. Rev. D86 (2012) 077504. arXiv:1206.3968, doi:10.1103/PhysRevD.86.077504.

[73] K. Chetyrkin, M. Steinhauser, Short distance mass of a heavy quark at order α_s^3, Phys. Rev. Lett. 83 (1999) 4001–4004. arXiv:hep-ph/9907509, doi:10.1103/PhysRevLett.83.4001.

[74] K. Chetyrkin, M. Steinhauser, The Relation between the $\overline{\mathrm{MS}}$ and the on-shell quark mass at order α_s^3, Nucl. Phys. B573 (2000) 617–651. arXiv:hep-ph/9911434, doi:10.1016/S0550-3213(99)00784-1.

[75] K. Melnikov, T. v. Ritbergen, The Three loop relation between the $\overline{\mathrm{MS}}$ and the pole quark masses, Phys. Lett. B482 (2000) 99–108. arXiv:hep-ph/9912391, doi:10.1016/S0370-2693(00)00507-4.

[76] Z.-z. Xing, H. Zhang, S. Zhou, Updated Values of Running Quark and Lepton Masses, Phys. Rev. D77 (2008) 113016. arXiv:0712.1419, doi:10.1103/PhysRevD.77.113016.